

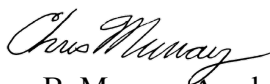
# AN ABSTRACT OF THE CAPSTONE REPORT OF

Yupeng Wu for the degree of Master of Chemical Sciences

Title: Synthesis and Optical Properties of Rare Earth Doped Fluorides Nanoparticles Via Enhanced Absorption

Project conducted at: Department of Chemistry  
University of Pennsylvania  
231 South 34th Street, Philadelphia, PA 19104  
Supervisor: Christopher B. Murray  
Dates of Project: May 15, 2018-May 9, 2019

Abstract approved:



Professor Christopher B. Murray, Academic Advisor

Rare-earth elements are strong candidates for upconverting materials due to their relatively long-lived excited states.<sup>1-3</sup> However, they are generally not efficient light absorbers.<sup>4-6</sup> One of the approaches to enhance the optical absorption is adding a sensitizer layer (*i.e.* an extra semiconductor layer or using organic dyes as sensitizer with stronger absorption properties).<sup>7</sup> On the other hand, the surface quenching effect decreases the efficiency of optical emission. This project explores the creation of undoped shells, sensitizer shells on rare earth nanoparticles and studies the effect of the size of the shell, semiconductor shells and dyes on the optical properties. NaYF<sub>4</sub>:Yb<sub>0.20</sub>, Er<sub>0.02</sub> nanoparticles are investigated specifically to reveal the effect of sensitizers on the absorption and emission properties. A solvothermal method is used to synthesize core NaYF<sub>4</sub>:Yb<sub>0.20</sub>, Er<sub>0.02</sub> nanoparticles and NaYF<sub>4</sub> doped core-undoped shell particles.<sup>8-13</sup> XRD and TEM indicated that pure  $\beta$ -NaYF<sub>4</sub> nanoparticles were synthesized. The size of NaYF<sub>4</sub> nanoparticles was monitored using reaction time. The emission spectrum revealed that growth of undoped NaYF<sub>4</sub> shells enhanced the emission intensity of doped core-undoped shell particles. This is presumably because the shell inhibits the nonradiative transition and the surface quenching on the surface of NaYF<sub>4</sub>:Yb<sub>0.20</sub>, Er<sub>0.02</sub> core nanoparticles. CdS shells and ligand exchange with a dye absorbing in NIR were investigated as potential methods to enhance the absorption properties of NaYF<sub>4</sub>:Yb<sub>0.20</sub>, Er<sub>0.02</sub> nanoparticles. TEM revealed that CdS segregated to form heterostructure with NaYF<sub>4</sub>:Yb<sub>0.20</sub>, Er<sub>0.02</sub> core nanoparticles instead of core-shell structure. This is likely due to the mismatch of CdS lattice to  $\beta$ -NaYF<sub>4</sub>. A NIR absorbing dye was coated to the NaYF<sub>4</sub>:Yb<sub>0.20</sub>, Er<sub>0.02</sub> core nanoparticles via ligand exchange method. A color change was noticed after the ligand exchange with the nanoparticles. However, the emission properties and energy transfer process need further studies since the intensity at 542 nm and 660 nm are not pronounced under 806 nm excitation and 980 nm excitation.

Synthesis and Optical Properties of Rare Earth Doped  
Fluorides Nanoparticles Via Enhanced Absorption

by  
Yupeng Wu

A CAPSTONE REPORT

submitted to the

University of Pennsylvania

in partial fulfillment of  
the requirements for  
the degree of

Master of Chemical Sciences

Presented on May 9, 2019  
Commencement on May 20, 2019

Master of Chemical Sciences Capstone Report of Yupeng Wu presented on May 9, 2019.

APPROVED:



---

*Christopher B. Murray, representing Inorganic Material Chemistry*

I understand that my Capstone Report will become part of the permanent collection of the University of Pennsylvania Master of Chemical Sciences Program. My signature below authorizes release of my final report to any reader upon request.



---

*Yupeng Wu, Author*

### **Acknowledgements**

This project was conducted at Prof. Christopher Murray's laboratory. I would like to thanks Prof. Murray for tremendous support and guidance in this project. Without him, I would not have the chance to start a project in material chemistry and adopt knowledges I have learned from several classes. Next, I would like to thanks post-doctoral fellow Guillaume Gouget for teaching me the TEM, fluorometry and countless advises throughout the project. Also, I would like to thanks Mingyue Zhang for teaching me the synthesis of core and core-shell nanoparticles. Last but not least, I would like to thanks all of the members at Prof. Murray's laboratory for their help and support in this project.

## Table of Contents

Abstract .....	i
Acknowledgements .....	iv
List of Figures .....	vi
List of Tables .....	viii
List of Appendices .....	ix
Introduction .....	1
Materials and Methods .....	5
Characterization .....	5
Synthesis of doped NaYF <sub>4</sub> :Yb <sub>0.20</sub> , Er <sub>0.02</sub> core nanoparticles .....	5
Synthesis of undoped NaYF <sub>4</sub> shell .....	6
Synthesis of CdS/NaYF <sub>4</sub> :Yb <sub>0.20</sub> , Er <sub>0.02</sub> nanoparticles .....	6
Synthesis of Dye/NaYF <sub>4</sub> :Yb <sub>0.20</sub> , Er <sub>0.02</sub> nanoparticles .....	6
Results and Discussion .....	7
Conclusion .....	18
Future Work .....	18
References .....	19
Appendices .....	22

## List of Figures

<b>Figure 1.</b> Energy transfer diagram of $\beta$ -NaYF <sub>4</sub> :Yb <sup>3+</sup> , Er <sup>3+</sup> . <sup>1</sup> .....	1
<b>Figure 2.</b> Sensitization process A) Light Absorption. B) Energy Transfer from Sensitizers to Core. C) Light Emission from Core. <sup>1</sup> .....	2
<b>Figure 3.</b> Target nanoparticles A) NaYF <sub>4</sub> :Yb <sub>0.20</sub> , Er <sub>0.02</sub> core nanoparticles; B) NaYF <sub>4</sub> /NaYF <sub>4</sub> :Yb <sub>0.20</sub> , Er <sub>0.02</sub> doped core-undoped shell nanoparticles; C) CdS/NaYF <sub>4</sub> :Yb <sub>0.20</sub> , Er <sub>0.02</sub> core-shell nanoparticles; D) dye/NaYF <sub>4</sub> :Yb <sub>0.20</sub> , Er <sub>0.02</sub> nanoparticles. <sup>1</sup> .....	3
<b>Figure 4.</b> Structure of IR-806 dye. <sup>28</sup> .....	4
<b>Figure 5.</b> A typical solvothermal reaction to synthesize a) NaYF <sub>4</sub> :Yb <sub>0.20</sub> , Er <sub>0.02</sub> ; b) NaYF <sub>4</sub> . <sup>21-22</sup> .....	7
<b>Figure 6.</b> TEM images of NaYF <sub>4</sub> :Yb <sub>0.20</sub> , Er <sub>0.02</sub> core nanoparticles with different reaction time. (A) 5 min (B) 15 min, average size 7 nm; (C) 25 min, average size 18 nm; (D) 27 mins, average size 20 nm; (E) 30 min, average size 22 nm.....	8
<b>Figure 7.</b> XRD pattern of NaYF <sub>4</sub> :Yb <sub>0.20</sub> , Er <sub>0.02</sub> core nanoparticles.....	9
<b>Figure 8.</b> TEM image of NaYF <sub>4</sub> core and doped core-undoped shell nanoparticles. (A) 18 nm NaYF <sub>4</sub> :Yb <sub>0.20</sub> , Er <sub>0.02</sub> core nanoparticles; (B) with 7 nm NaYF <sub>4</sub> undoped shell; (C) with 10 nm NaYF <sub>4</sub> undoped shell; (D) with 12 nm NaYF <sub>4</sub> undoped shell; (E) with 17 nm NaYF <sub>4</sub> undoped shell. ....	10
<b>Figure 9.</b> XRD pattern of NaYF <sub>4</sub> doped core-undoped shell nanoparticles. ....	11
<b>Figure 10.</b> Absorption spectrum of NaYF <sub>4</sub> doped core-undoped shell nanoparticles dispersed in hexane.....	12
<b>Figure 11.</b> Emission spectrum of NaYF <sub>4</sub> :Yb <sub>0.20</sub> , Er <sub>0.02</sub> core nanoparticles and NaYF <sub>4</sub> doped core-undoped shell nanoparticles under 980 nm excitation. a) Up-conversion fluorescence under the 980 nm excitation; b) Up-conversion fluorescence intensity with respect of shell thickness. ....	13
<b>Figure 12.</b> Synthesis of CdS/NaYF <sub>4</sub> :Yb <sub>0.20</sub> , Er <sub>0.02</sub> . <sup>24-26</sup> .....	14
<b>Figure 13.</b> TEM image of CdS/NaYF <sub>4</sub> :Yb <sub>0.20</sub> , Er <sub>0.02</sub> nanoparticles. ....	14
<b>Figure 14.</b> Absorption spectrum of CdS/NaYF <sub>4</sub> :Yb <sub>0.20</sub> , Er <sub>0.02</sub> heterostructure dispersed in hexane. ....	15
<b>Figure 15.</b> Emission spectrum of 18 nm NaYF <sub>4</sub> :Yb <sub>0.20</sub> , Er <sub>0.02</sub> core and CdS/NaYF <sub>4</sub> :Yb <sub>0.20</sub> , Er <sub>0.02</sub> system under the 980 nm excitation. ....	16

- Figure 16.** Absorption spectrum of IR-806 dye dissolved in 3:1 solvent of isopropanol and ethanol, and dye/ $\text{NaYF}_4\text{:Yb}_{0.20}\text{, Er}_{0.02}$  nanoparticles dispersed in same solvent. .... 16
- Figure 17.** Emission spectrum of dye/ $\text{NaYF}_4\text{:Yb}_{0.20}\text{, Er}_{0.02}$  nanoparticles (red) and 18 nm  $\text{NaYF}_4\text{:Yb}_{0.20}\text{, Er}_{0.02}$  core nanoparticles (black) under the 804 nm excitation..... 17

## List of Tables

<b>Table 1.</b> Average diameter and average width of 18 nm NaYF <sub>4</sub> :Yb <sub>0.20</sub> , Er <sub>0.02</sub> core nanoparticles and NaYF <sub>4</sub> doped core-undoped shell nanoparticles. ....	11
--	----



## List of Appendices

<b>Appendix 1.</b> TEM images of 18 nm core NaYF <sub>4</sub> :Yb <sub>0.20</sub> , Er <sub>0.02</sub> core nanoparticles. ....	22
<b>Appendix 2.</b> TEM images of 20 nm core NaYF <sub>4</sub> :Yb <sub>0.20</sub> , Er <sub>0.02</sub> core nanoparticles. ....	22
<b>Appendix 3.</b> TEM images of 22 nm core NaYF <sub>4</sub> :Yb <sub>0.20</sub> , Er <sub>0.02</sub> core nanoparticles. ....	22
<b>Appendix 4.</b> TEM images of 25 nm NaYF <sub>4</sub> doped core-undoped shell nanoparticles. ...	23
<b>Appendix 5.</b> TEM images of 28 nm NaYF <sub>4</sub> doped core-undoped shell nanoparticles. ...	23
<b>Appendix 6.</b> TEM images of 30 nm NaYF <sub>4</sub> doped core-undoped shell nanoparticles. ...	23
<b>Appendix 7.</b> TEM images of 35 nm NaYF <sub>4</sub> doped core-undoped shell nanoparticles. ...	24
<b>Appendix 8.</b> TEM images of CdS/NaYF <sub>4</sub> :Yb <sub>0.20</sub> , Er <sub>0.02</sub> nanoparticles. ....	24
<b>Appendix 9.</b> TEM images of Dye/NaYF <sub>4</sub> :Yb <sub>0.20</sub> , Er <sub>0.02</sub> nanoparticles after ligand exchange .....	24
<b>Appendix 10.</b> Emission spectra of NaYF <sub>4</sub> :Yb <sub>0.20</sub> , Er <sub>0.02</sub> core nanoparticles. ....	25
<b>Appendix 11.</b> Hexane suspension of 18 nm NaYF <sub>4</sub> :Yb <sub>0.20</sub> , Er <sub>0.02</sub> core nanoparticles (left); Hexane suspension of CdS/NaYF <sub>4</sub> :Yb <sub>0.20</sub> , Er <sub>0.02</sub> (right).....	25
<b>Appendix 12.</b> Hexane suspension of 18 nm NaYF <sub>4</sub> :Yb <sub>0.20</sub> , Er <sub>0.02</sub> core nanoparticles (left); IR-806 dye dissolved in 3:1 solvent of isopropanol and ethanol (middle); Dye/NaYF <sub>4</sub> :Yb <sub>0.20</sub> , Er <sub>0.02</sub> nanoparticles dispersed in toluene (right) .....	25

## Introduction

The rare earth elements have unique optical, catalytic, and magnetic properties because of their 4f, 5p, and 5d electrons.<sup>1-3</sup> Research has shown that most rare earth elements have relatively long-lived excited states (10  $\mu$ s-10 ms) because their 4f electron configurations generates various well-defined electronic levels.<sup>1-3</sup> The long-lived excited states allow the sequential absorption of two or more photons, and emit a single photon whose energy is greater than the energy of absorbed photons.<sup>1-4</sup> This process is called up-conversion (UC) process.<sup>1-4</sup> The up-conversion process can be divided into three subclasses by the energy transfer mechanism: excited state absorption (ESA); energy transfer up-conversion (ETU); and photon avalanche (PA).<sup>5-7</sup> In the ESA mechanism, two laser pumping processes are needed, while one laser pumping excites the ion from ground state to first excited state, and the other laser pumping excites the ion from first excited state to the second excited state.<sup>5</sup> In the ETU mechanism, one laser pumping is needed.<sup>5</sup> The laser pumping first excites the sensitizer ion from ground state to the excited state.<sup>5</sup> Then, the sensitizer excites the activator to excited state via energy transfer process.<sup>5</sup> Materials with up-conversion luminescence characteristics have shown potential in various optical applications, such as solid-state lasers, low-intensity IR imaging, sensitive bio-probes, and bio-imaging.<sup>5</sup> The up-conversion property, along with inherent low toxicity, provides opportunities for rare earth elements to be used in up-conversion luminescent materials for optics, electronics, photovoltaics, and medical sensor.<sup>1, 2, 5, 6</sup>

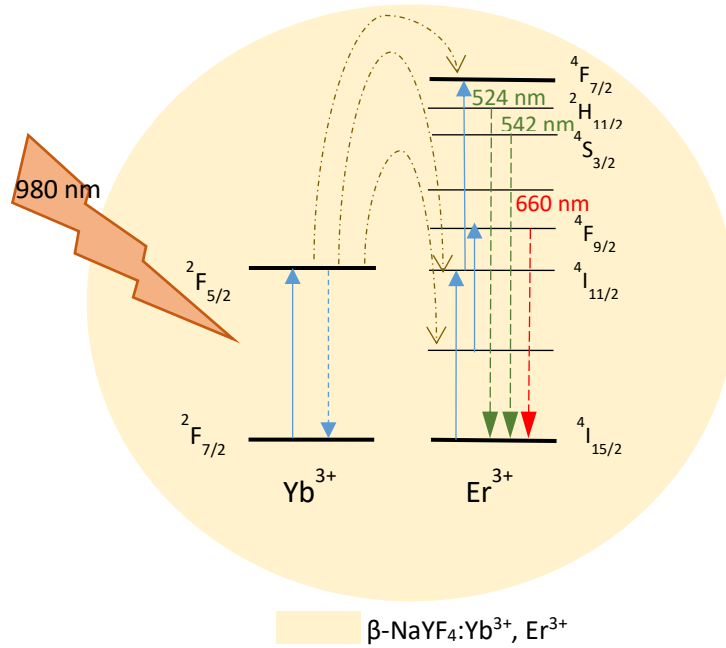


**Figure 1.** Energy transfer diagram of  $\beta$ -NaYF<sub>4</sub>:Yb<sup>3+</sup>, Er<sup>3+</sup>.<sup>1</sup>

Among various upconverting materials,  $\beta$ -NaYF<sub>4</sub>:Yb<sup>3+</sup>, Er<sup>3+</sup> is one of the most efficient materials under near infrared (NIR) excitation.<sup>3-5</sup> The energy transfer of  $\beta$ -NaYF<sub>4</sub>:Yb<sup>3+</sup>, Er<sup>3+</sup> is shown in **Figure 1**. The 980 nm light excites Yb<sup>3+</sup> ion from  $^2F_{7/2}$  ground state to  $^2F_{5/2}$  excited state via absorption.<sup>3-8</sup> Then, Er<sup>3+</sup> ion is excited to high energy state by Yb<sup>3+</sup> ion via energy transfer. When Er<sup>3+</sup> ion relaxes, it emits photons at three wavelengths: 524 nm, 542 nm and 660 nm, corresponding to energy diagram levels

of 4f-4f transitions as shown in **Figure 1**.<sup>3-9</sup> In the energy transfer process, the amount of IR photons absorbed by  $\text{Yb}^{3+}$  is more than the amount of visible photons emitted by  $\text{Er}^{3+}$ .<sup>3-9</sup>

Current research has shown that lanthanide doped fluorides, such as  $\text{NaYF}_4$ : 20%  $\text{Yb}^{3+}$ , 2%  $\text{Er}^{3+}$ , are the most efficient nanomaterials for up-conversion photoluminescence.<sup>5,6</sup> However, the efficiency of energy transfer in  $\beta\text{-NaYF}_4\text{:Yb}^{3+}$ ,  $\text{Er}^{3+}$  is still very low due to surface quenching effect and low absorption of rare earth elements.<sup>3,4,7</sup> Thus, it is desired to suppress surface quenching effect by adding a shell or enhance the absorption by adding sensitizers, such as semiconductors or dyes. The sensitization process is shown by **Figure 2**.

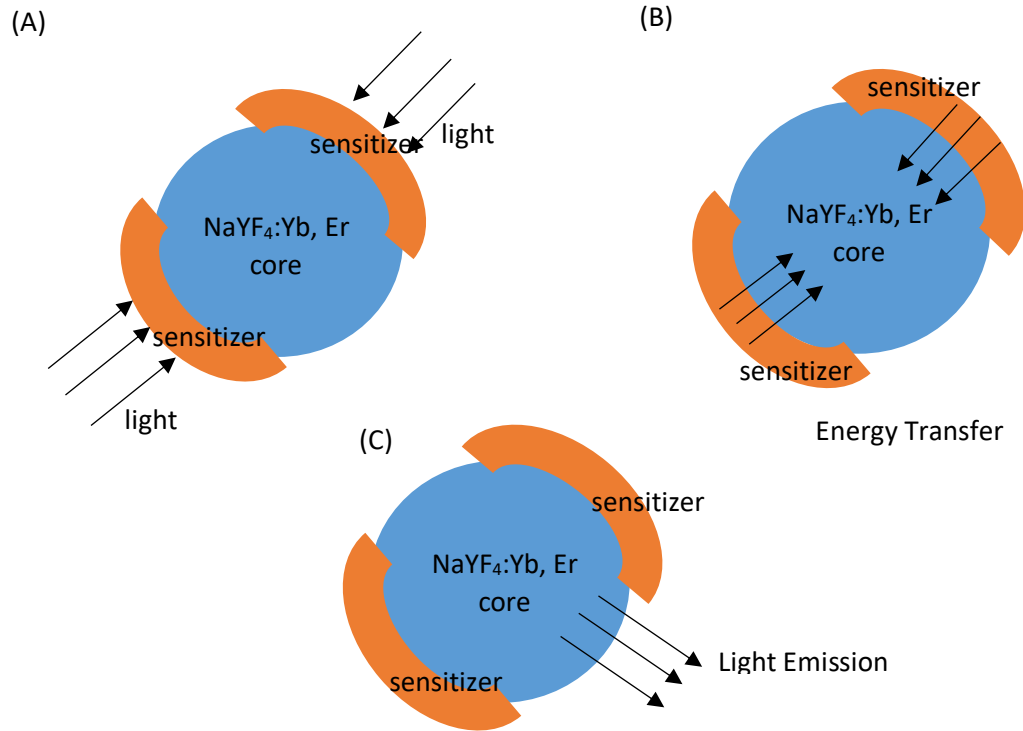


**Figure 2.** Sensitization process A) Light Absorption. B) Energy Transfer from Sensitizers to Core. C) Light Emission from Core.<sup>1</sup>

During the sensitization process, the sensitizer absorbs lower energy photons and reaches to the excited state (**Figure 2A**).<sup>4</sup> Then, it performs a non-radiative energy transfer to excite the core, as shown in **Figure 2B**.<sup>4</sup> Eventually, the core emits a light and relax to ground state, as shown in **Figure 2C**.<sup>4</sup> The energy transfer can occur as long as the sensitizer is doped in the crystal structure or attached to the core.<sup>4,7</sup>

The goal of this project is to first explore the formation of undoped shell and sensitizers, such as semiconductor shells and dyes, on rare earth core nanoparticles; and then, studies the effect of the size of the shell, dyes and semiconductor shells on the optical properties. Firstly,  $\text{NaYF}_4\text{:Yb}_{0.20}$ ,  $\text{Er}_{0.02}$  core nanoparticles (**Figure 3A**) are synthesized. Secondly, the core nanoparticles are used to synthesize  $\text{NaYF}_4/\text{NaYF}_4\text{:Yb}_{0.20}$ ,  $\text{Er}_{0.02}$  doped core-undoped shell nanoparticles (**Figure 3B**),  $\text{CdS}/\text{NaYF}_4\text{:Yb}_{0.20}$ ,  $\text{Er}_{0.02}$  core-shell nanoparticles (**Figure 3C**), and

dye/NaYF<sub>4</sub>:Yb<sub>0.20</sub>, Er<sub>0.02</sub> nanoparticles (**Figure 3D**). Thirdly, the optical properties of these nanoparticles are studied via absorption and emission spectrum.

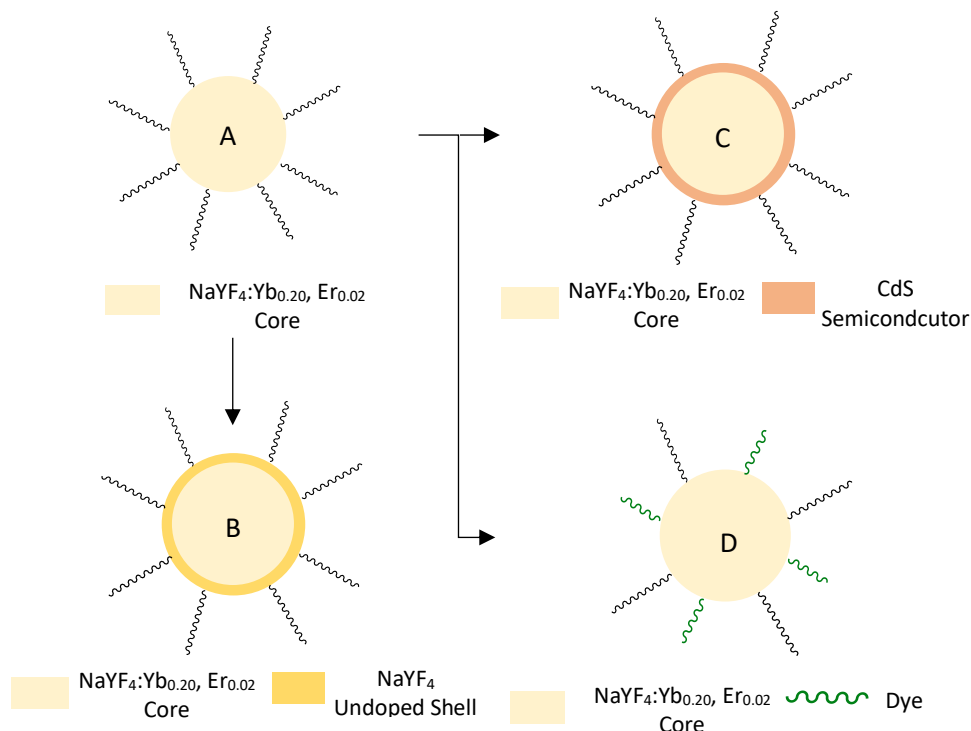


**Figure 3.** Target nanoparticles A) NaYF<sub>4</sub>:Yb<sub>0.20</sub>, Er<sub>0.02</sub> core nanoparticles; B) NaYF<sub>4</sub>/NaYF<sub>4</sub>:Yb<sub>0.20</sub>, Er<sub>0.02</sub> doped core-undoped shell nanoparticles; C) CdS/NaYF<sub>4</sub>:Yb<sub>0.20</sub>, Er<sub>0.02</sub> core-shell nanoparticles; D) dye/NaYF<sub>4</sub>:Yb<sub>0.20</sub>, Er<sub>0.02</sub> nanoparticles.<sup>1</sup>

There are several methods to synthesize rare-earth nanocrystals. Hydrothermal methods require high pressure vessels and relatively long reaction time, which makes it difficult to optimize the growth of nanoparticles.<sup>10-13</sup> At room temperature, ionothermal and microemulsion methods have been developed.<sup>14-18</sup> These methods use reactive precursors in immiscible solvents and rely on sonication or vigorous stirring for nucleation and growth of nanocrystals.<sup>14-18</sup> Solvothermal method uses high boiling point non-aqueous solvents to overcome thermodynamic barrier between crystal structures and shorten the reaction time so that the parameters can be tuned to optimize the nucleation and growth of nanocrystals.<sup>13,19,20</sup>

The NaYF<sub>4</sub>:Yb<sub>0.20</sub>, Er<sub>0.02</sub> core nanoparticles and undoped NaYF<sub>4</sub> shell will be synthesis via the solvothermal method because of the relatively short reaction time and tunability of parameters. The reactions use rare earth chloride salts as precursors to enable control over monodispersity and size of the rare-earth nanoparticle.<sup>9, 21, 22</sup> The reaction time determines the size of the nanoparticles in the growth solution.<sup>21-23</sup> Another solvothermal method was chosen for CdS shell synthesis because of short reaction time and tunability of parameters. The reactions use cadmium oxide and trioctylphosphine sulfide as precursors to enable formation of CdS.<sup>24-26</sup>

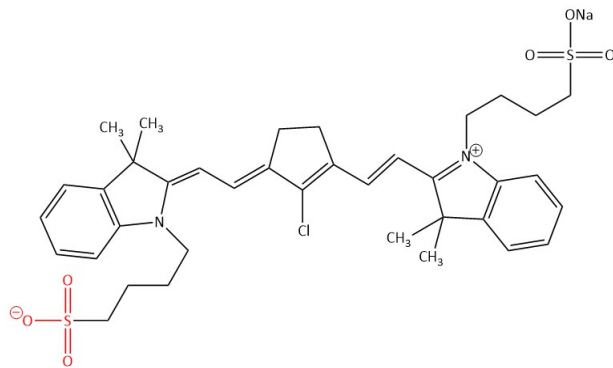


**Figure 4.** Structure of IR-806 dye.<sup>28</sup>

A ligand exchange will be used to synthesize dye-coated NaYF<sub>4</sub>:Yb<sub>0.20</sub>, Er<sub>0.02</sub> core nanoparticles.<sup>27</sup> IR-806 dye was chosen for the dye-coated system for three reasons (**Figure 4**). Firstly, the sulfonate group, highlighted in red, is a promising binding group to the surface of NaYF<sub>4</sub>:Yb<sub>0.20</sub>, Er<sub>0.02</sub> core nanoparticles. Secondly, the absorption of IR-806 dye is 803 – 809 nm, which was different than the reported absorption of Yb<sup>3+</sup> ion (980 nm) in the NaYF<sub>4</sub>:Yb<sub>0.20</sub>, Er<sub>0.02</sub> core nanoparticles.<sup>29</sup> The absorption difference distinguishes the absorption of the dye and Yb<sup>3+</sup> ion. Lastly, relatively short alkyl chains have higher possibilities to transfer energy to the surface of NaYF<sub>4</sub>:Yb<sub>0.20</sub>, Er<sub>0.02</sub> core nanoparticles.<sup>30-31</sup>

## Materials and Methods

### Chemicals

Chemicals that are used in the project are all purchased from Fisher Chemicals and Sigma Aldrich. In the synthesis, the rare earth precursors are provided by rare earth chloride salt. Yttrium (III) chloride hexahydrate (99.999%) is purchased from Fisher Chemicals. Erbium (III) chloride hexahydrate (99.999%) and ytterbium (III) chloride hexahydrate (99.9%) are purchased from Sigma Aldrich. The sodium and fluoride precursors are provided by sodium hydroxide and ammonium fluoride. Sodium hydroxide (99.9%) and ammonium fluoride (99.9%) are purchased from Fisher Chemical. Oleic Acid (OA, 90%) and 1-Octadecene (ODE, 90%, technical grade) are both purchased from Sigma Aldrich. In the CdS synthesis, trioctylphosphine sulfide (TOPS), which is the sulfur precursor, is premade in the laboratory with a concentration of 1M. Liquid trioctylphosphine (TOP) is pre-prepared in the laboratory. Solid trioctylphosphine oxide (TOPO) (97%) and cadmium oxide (99.99%) are purchased from Sigma Aldrich. The IR-806 dye used in the synthesis is purchased from Sigma Aldrich. All of the purchased chemicals were used without further purification. Solvents were ACS grade or higher.

### Characterization

All of the TEM imaging was performed on a JEOL JEM-1400 transmission electron microscopy (TEM) at 120 V and a magnitude of 30k - 50k. The absorption measurement was performed by an Agilent Cary 5000 UV-vis-NIR absorption spectrometer. For each NaYF<sub>4</sub> sample, the absorption scans from 1050 nm to 200 nm with baseline correction. For dye, dye-coated NaYF<sub>4</sub>:Yb<sub>0.20</sub>, Er<sub>0.02</sub> and CdS/NaYF<sub>4</sub>:Yb<sub>0.20</sub>, Er<sub>0.02</sub>, each scan was from 1200 nm to 200 nm with baseline correction. The room temperature up conversion emission spectrum was performed on an Edinburgh Instruments FLS 1000 fluorometry using a Xe 1200 light as the excitation source and PMT980 as detector. For all of the scans, the scan slit was set as 4 nm and offset slit was set as 2 nm. For NaYF<sub>4</sub>, each scan was performed under 980 nm excitation and detected from 500 nm to 700 nm with dwell time of 10 seconds. For dye coated sample, 2 different scans are performed. One of the scans is excited at 804 nm while the other is excited at 980 nm. The XRD is performed on a Rigaku SmartLab X-ray diffractometer with Cu K $\alpha$  radiation ( $\lambda = 1.5416 \text{ \AA}$ ) at 40 kV and 30 mA with guidance software.

### Synthesis of doped NaYF<sub>4</sub>:Yb<sub>0.20</sub>, Er<sub>0.02</sub> core nanoparticles

In a 50 mL centrifuge tube, approximately yttrium (III) chloride (0.471 g, 1.32 mmol), ytterbium (III) chloride (0.157 g, 0.4 mmol), and erbium (III) chloride (0.0155 g, 0.04 mmol) are dissolved in 10 mL methanol.<sup>10</sup> Oleic acid (12 mL), and 1-octadecene (30 mL) were then added to the same centrifuge tube as the ligand and reaction solvent respectively.<sup>21,23</sup> This formed the mixture A. The mixture A was then added to 125 mL 3-neck flask and heated to 150 °C for 30 minutes under the vacuum. After heating, the mixture A was cooled to room temperature. Meanwhile, sodium hydroxide (0.200 g, 5 mmol) and ammonium fluoride (0.296 g, 8 mmol) were added to another 50 mL centrifuge tube and dissolved in 10 mL methanol, which formed mixture B.<sup>21,23</sup> At room temperature, mixture B was added into mixture A and stirred for 60 minutes to form mixture C. Then, mixture C was degassed at 110 °C for 30 minutes. After degassing, the mixture C was heated in salt bath to 320 °C under the N<sub>2</sub>.<sup>22</sup> In order to make core nanoparticles with

different sizes, the reaction times were set to 5 minutes, 10 minutes, 15 minutes, 20 minutes, 25 minutes and 30 minutes. Once the reaction time reached, the solution was cooled to room temperature and washed by hexane and ethanol for three times to allow core nanoparticles to precipitate and further disperse in hexane. For each sample, the precipitated NaYF<sub>4</sub>:Yb<sub>0.20</sub>, Er<sub>0.02</sub> core nanoparticles were dispersed in 10 mL of hexane to make NaYF<sub>4</sub>:Yb<sub>0.20</sub>, Er<sub>0.02</sub> core nanoparticles mother suspension.

#### **Synthesis of undoped NaYF<sub>4</sub> shell**

The NaYF<sub>4</sub> shell synthesis is similar to the synthesis procedure for NaYF<sub>4</sub>:Yb<sub>0.20</sub>, Er<sub>0.02</sub> core nanoparticles. In a 50 mL centrifuge tube, yttrium chloride salt was dissolved in methanol and mixed with OA and ODE to form mixture D.<sup>21</sup> The mixture D was then degassed at 150 °C for 30 minutes in a 125 mL 3-neck flask. After heating, the mixture D was cooled down to room temperature and mixed with a methanol solution of sodium hydroxide and ammonium fluoride to form mixture E.<sup>21,22</sup> After stirring for 60 minutes, the mixture E is degassed at 110 °C for 30 minutes. After degassing, the flask was filled with N<sub>2</sub> for 2 minutes at 110 °C. Then, the NaYF<sub>4</sub>:Yb<sub>0.20</sub>, Er<sub>0.02</sub> core hexane suspension was injected to the mixture E at 110 °C to form mixture F. After injection, the mixture F was degassed at 110 °C for 30 minutes before it was heated in salt bath to 320 °C under the N<sub>2</sub> for 30 minutes.<sup>22</sup> After the reaction, the solution was cooled to room temperature and washed by hexane and ethanol for three times to allow nanoparticles to disperse in hexane. Each sample was dispersed in 10 mL of hexane to make hexane suspension of NaYF<sub>4</sub> doped core-undoped shell nanoparticles. In this reaction, the initial reactant inputs were calculated with the respect of the desired core-shell nanoparticle size.

#### **Synthesis of CdS/NaYF<sub>4</sub>:Yb<sub>0.20</sub>, Er<sub>0.02</sub> nanoparticles**

CdO powder (0.060 g, 0.47 mmol), TOPO (6.000 g, 15.52 mmol) and oleic acid (0.8 mL) were added to a 3-neck flask and heated up to 340 °C under N<sub>2</sub> for 30 minutes.<sup>24-26</sup> The color change of the solution (from red to clear) indicates that CdO dissolved in TOPO and forms Cd precursor.<sup>24,25</sup> The mixture was then cooled to 150 °C. After injecting 0.200 mL NaYF<sub>4</sub>:Yb<sub>0.20</sub>, Er<sub>0.02</sub> core hexane suspension, the mixture was kept at 150 °C under vacuum for 60 minutes. After degassing, the mixture was heated to 350 °C under the nitrogen.<sup>24-26</sup> At 320 °C, TOP (3.5 mL) was injected into the flask.<sup>24-26</sup> Pre-prepared TOPS and TOP (1 mL) were injected into the mixture at 330 °C.<sup>24-26</sup> The flask was kept at 350 °C for 3 minutes for the grow of CdS. Once the reaction time reached, the solution was washed with toluene and acetone for three times to allow nanoparticles to disperse in hexane.

#### **Synthesis of Dye/NaYF<sub>4</sub>:Yb<sub>0.20</sub>, Er<sub>0.02</sub> nanoparticles**

The IR-806 dye was dissolved in ethanol. Hexane (3 mL) was added to an aliquot of NaYF<sub>4</sub>:Yb<sub>0.20</sub>, Er<sub>0.02</sub> core nanoparticle mother suspension (2 mL) to obtain 5 mL of diluted suspension of NaYF<sub>4</sub>:Yb<sub>0.20</sub>, Er<sub>0.02</sub>. The NaYF<sub>4</sub>:Yb<sub>0.20</sub>, Er<sub>0.02</sub> suspension (5 mL) then was added into 5 mL of dye solution. The mixture was shaken gently and then stirred for 60 minutes.<sup>27</sup> The mixture was washed by hexane and ethanol to allow the dye/NaYF<sub>4</sub>:Yb<sub>0.20</sub>, Er<sub>0.02</sub> nanoparticles to be dispersed in 3:1 alcohol solution of isopropanol and ethanol.

## Results and Discussion

NaYF<sub>4</sub>:Yb<sub>0.20</sub>, Er<sub>0.02</sub> core nanoparticles were synthesized by solvothermal method with controlled sizes and quality (**Figure 5a**). Rare-earth, sodium, and fluoride precursors were heated to 320 °C in ODE in the presence of OA, a ligand to control the dispersion of nanoparticles. Different reaction times were applied to tune the sizes of core nanoparticles. TEM characterizations were used to characterize the morphology and sizes of the NaYF<sub>4</sub>:Yb<sub>0.20</sub>, Er<sub>0.02</sub> core nanoparticles, as shown in **Figure 6**. XRD was performed to determine the crystalline phase of the nanoparticle as shown in **Figure 7**.

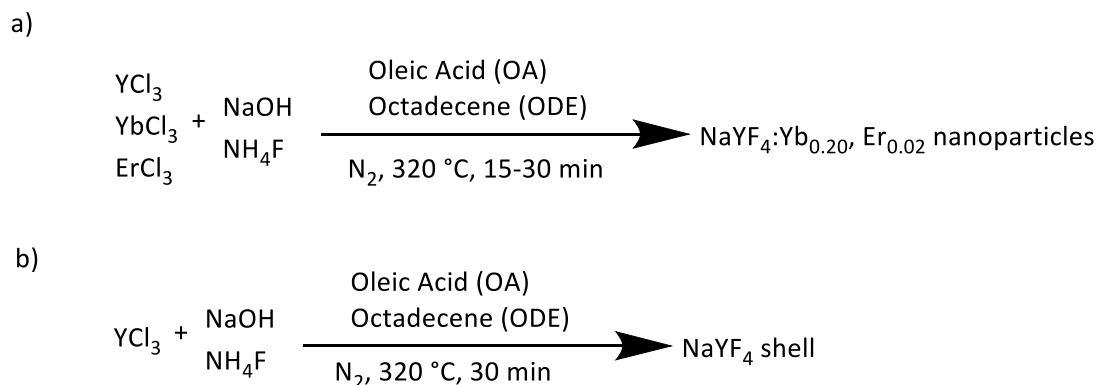


**Figure 5.** A typical solvothermal reaction to synthesize a) NaYF<sub>4</sub>:Yb<sub>0.20</sub>, Er<sub>0.02</sub>; b) NaYF<sub>4</sub><sup>21-22</sup>

When the reaction time was set to 5 minutes, there was no noticeable nanocrystal in the solution, as shown in **Figure 6A**. As the reaction time increased to 15 minutes, small particles started to be observed with a size of  $7.2 \pm 0.5$  nm, as seen in **Figure 6B**. When reaction time further increased to 25, 27 and 30 minutes, the particle grew bigger as seen in **Figure 6C-E**. The average sizes of the core nanoparticles were  $18.3 \pm 1.4$  nm,  $20.3 \pm 1.3$  nm,  $22.2 \pm 1.7$  nm, which corresponded to reaction times of 25 minutes, 27 minutes and 30 minutes respectively. As the time increase to 30 minutes, a hexagonal morphology started to be observed, as seen in **Figure 6E**. This morphology was expected for  $\beta$ -NaYF<sub>4</sub>:Yb<sub>0.20</sub>, Er<sub>0.02</sub> nanoparticles as its crystal structure was hexagonal.<sup>27,31</sup> The XRD pattern in **Figure 7** confirmed only  $\beta$ -NaYF<sub>4</sub>:Yb<sub>0.20</sub>, Er<sub>0.02</sub> nanoparticles existed in the synthesized core system as all the diffraction peaks could be indexed to a pure beta phase NaYF<sub>4</sub> crystal based on standard data from ICSD database (ICSD\_CollCode259178).<sup>32</sup>



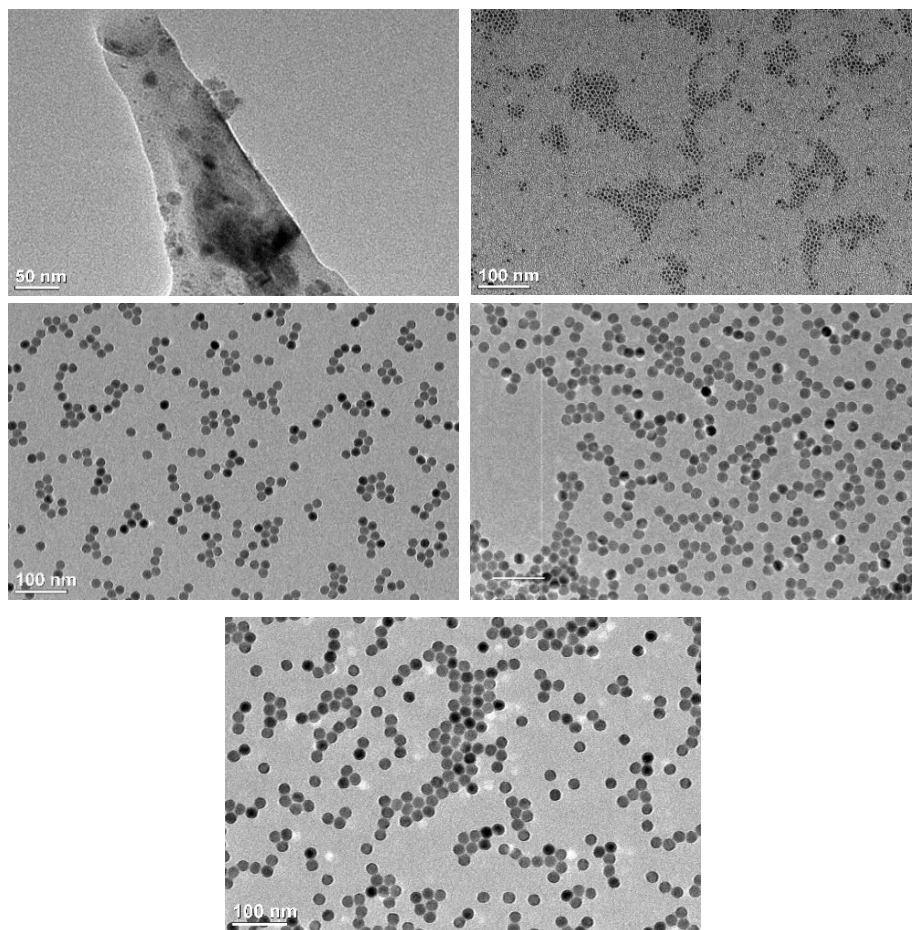


**Figure 6.** TEM images of NaYF<sub>4</sub>:Yb<sub>0.20</sub>, Er<sub>0.02</sub> core nanoparticles with different reaction time. (A) 5 min (B) 15 min, average size 7 nm; (C) 25 min, average size 18 nm; (D) 27 mins, average size 20 nm; (E) 30 min, average size 22 nm.

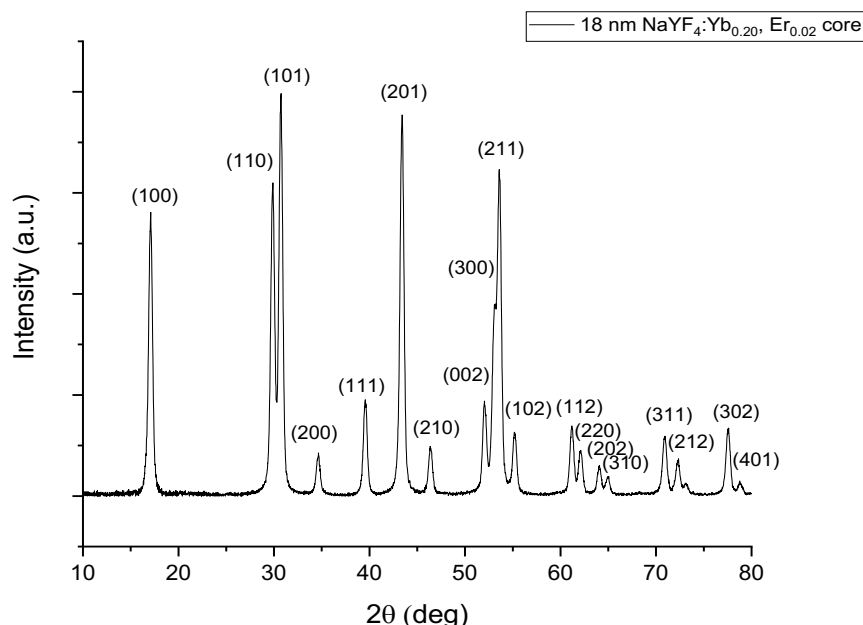


**Figure 7.** XRD pattern of NaYF<sub>4</sub>:Yb<sub>0.20</sub>, Er<sub>0.02</sub> core nanoparticles.

To investigate the effect of shell thickness to the optical properties of NaYF<sub>4</sub>:Yb<sub>0.20</sub>, Er<sub>0.02</sub> core nanoparticles, four different sizes of shell were grown on the 18 nm core nanoparticles. A similar solvothermal method was used to synthesize undoped NaYF<sub>4</sub> shell on top of NaYF<sub>4</sub>:Yb<sub>0.20</sub>, Er<sub>0.02</sub> core nanoparticles (**Figure 5b**). After injecting NaYF<sub>4</sub>:Yb<sub>0.20</sub>, Er<sub>0.02</sub> core nanoparticles, yttrium, sodium, and fluoride precursors were heated to 320 °C in ODE in the presence of OA, a ligand to control the dispersion of nanoparticles. TEM images in **Figure 8A** showed the original 18 nm cores, while **Figure 8B-E** showed the core-shell particles with 7 nm, 10 nm, 12 nm, and 17 nm shells respectively. XRD was performed to investigate the crystalline phase of NaYF<sub>4</sub> doped core-undoped shell nanoparticles, as shown in **Figure 9**.

**Table 1** summarizes the sizes of 18 nm NaYF<sub>4</sub>:Yb<sub>0.20</sub>, Er<sub>0.02</sub> core nanoparticles and NaYF<sub>4</sub> doped core-undoped shell nanoparticles which were presented in **Figure 9**. The sizes of the core-shell nanoparticles were measured in two dimensions due to the geometry of hexagonal prisms. As shown in **Table 1**, the average particle diameter was  $24.6 \pm 1.4$  nm,  $27.8 \pm 1.8$  nm,  $30.4 \pm 2.1$  nm, and  $35.6 \pm 2.4$  nm respectively, which corresponding to **Figure 9B-E** respectively. In **Figure 9A**, the 18 nm core nanoparticles had a less pronounced hexagonal morphology. As the shell grows, the nanoparticles started to have a more obvious hexagonal morphology. In **Figure 9B-C**, nanoparticles were clearly hexagons. In **Figure 9D-E**, the rectangular morphology was the side of hexagonal prisms. To ensure the core-shell nanoparticles were in the beta phase, XRD was performed. As shown in **Figure 10**, all of the peaks could be assigned to beta phase NaYF<sub>4</sub> crystal based on standard data from ICSD database (ICSD\_CollCode259178), which indicated that core-shell nanoparticles stayed in beta phase.<sup>32</sup> The TEM characterization and XRD pattern indicated that the shell successfully grew on the doped NaYF<sub>4</sub>:Yb<sub>0.20</sub>, Er<sub>0.02</sub> core nanoparticles and did not deform into the alpha phase.

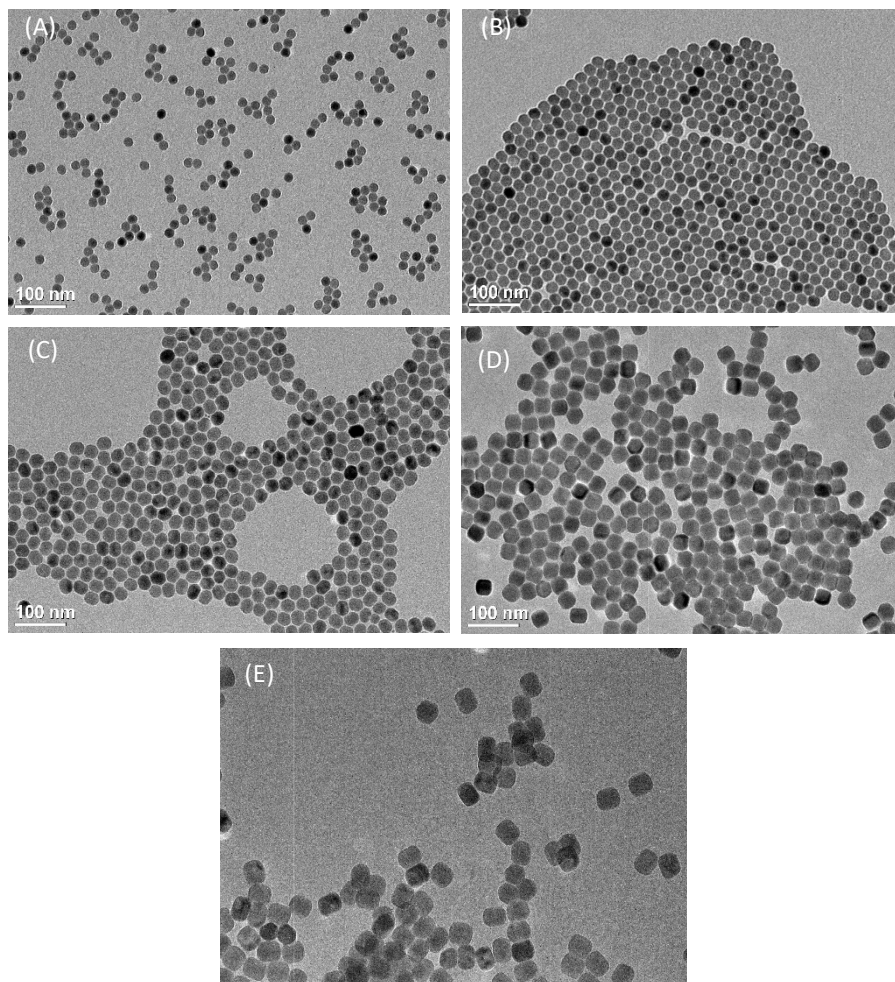


**Figure 8.** TEM image of NaYF<sub>4</sub>:Yb<sub>0.20</sub>, Er<sub>0.02</sub> core and NaYF<sub>4</sub> doped core-undoped shell nanoparticles. (A) 18 nm NaYF<sub>4</sub>:Yb<sub>0.20</sub>, Er<sub>0.02</sub> core nanoparticles; (B) with 7 nm NaYF<sub>4</sub> undoped shell; (C) with 10 nm NaYF<sub>4</sub> undoped shell; (D) with 12 nm NaYF<sub>4</sub> undoped shell; (E) with 17 nm NaYF<sub>4</sub> undoped shell.

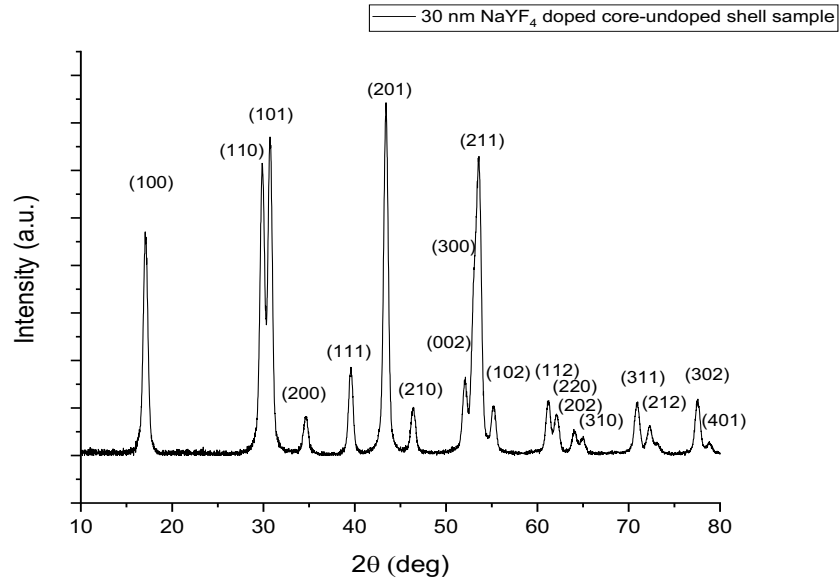


**Figure 9.** XRD pattern of NaYF<sub>4</sub> doped core-undoped shell nanoparticles.

**Table 1.** Average diameter and average width of 18 nm NaYF<sub>4</sub>:Yb<sub>0.20</sub>, Er<sub>0.02</sub> core nanoparticles and NaYF<sub>4</sub> doped core-undoped shell nanoparticles.

	Avg. Diameter	Avg. Width
core	18.3 nm	
7 nm shell	24.6 nm	22.8 nm
10 nm shell	27.8 nm	24.5 nm
12 nm shell	30.4 nm	27.4 nm
17 nm shell	35.6 nm	31.7 nm

The optical properties of NaYF<sub>4</sub> core-shell nanoparticles were investigated at room temperature. **Figure 10** and **Figure 11** showed the absorption and emission spectra of synthesized NaYF<sub>4</sub> doped core-undoped shell nanoparticles.

The absorption spectrum of NaYF<sub>4</sub> doped core-undoped shell nanoparticles measured the range of 400 nm to 1200 nm (**Figure 10**). One sharp peak at 974 nm and three weak peaks at 528 nm, 542 nm, and 660 nm were observed in the absorption spectrum. The sharp absorption peak at 974 nm corresponds to the absorption of Yb<sup>3+</sup> ion from <sup>2</sup>F<sub>7/2</sub> ground state to <sup>2</sup>F<sub>5/2</sub> excited state.<sup>3-8</sup> The weak absorption peaks at 528 nm and 660 nm correspond to the absorption of Er<sup>3+</sup> ion from low energy <sup>4</sup>I<sub>15/2</sub> state to <sup>2</sup>H<sub>11/2</sub> and <sup>4</sup>F<sub>9/2</sub> excited states respectively.<sup>3-8</sup> The weak absorption peak at 377 nm corresponds to the absorption of Er<sup>3+</sup> from <sup>4</sup>G<sub>11/2</sub> to <sup>4</sup>F<sub>9/2</sub>.<sup>11,13</sup> The absorption spectrum indicated that the Yb<sup>3+</sup> and Er<sup>3+</sup> were effectively doped in the NaYF<sub>4</sub> crystal lattice. Before measuring emission spectra, all the samples were diluted until the peak intensity reached 0.052 AU at 974 nm.

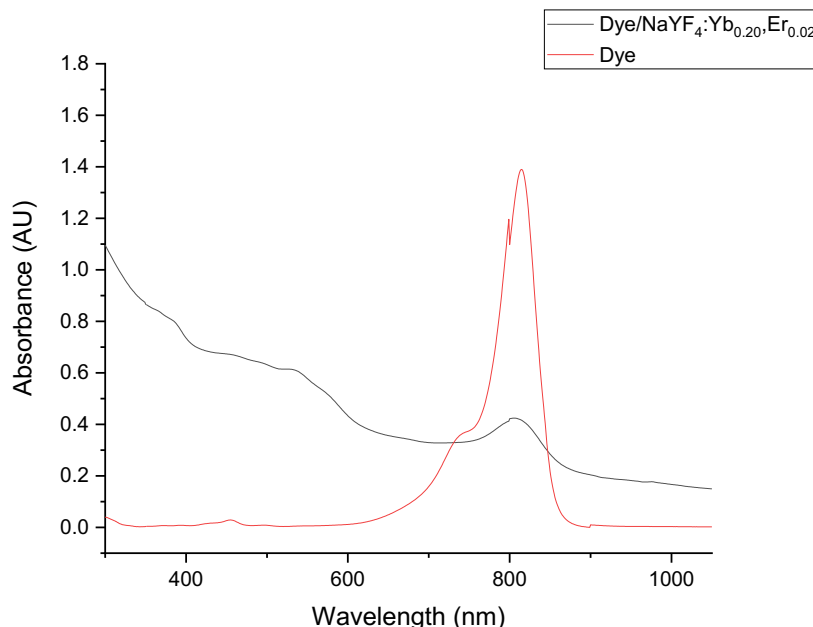


**Figure 10.** Absorption spectrum of NaYF<sub>4</sub> doped core-undoped shell nanoparticles dispersed in hexane.

**Figure 11** illustrates the up-conversion emission spectra of different size nanoparticles under 980 nm excitation. All of the spectra were measured at room temperature. The 980 nm light excited the Yb<sup>3+</sup> from <sup>2</sup>F<sub>7/2</sub> ground state to <sup>2</sup>F<sub>5/2</sub> excited state. The emission peaks were found at 528 nm, 542 nm, and 656 nm, which corresponded to three relaxation process of Er<sup>3+</sup>: <sup>2</sup>H<sub>11/2</sub>→<sup>4</sup>I<sub>15/2</sub>, <sup>4</sup>S<sub>3/2</sub>→<sup>4</sup>I<sub>15/2</sub>, and <sup>4</sup>F<sub>9/2</sub>→<sup>4</sup>I<sub>15/2</sub> respectively.<sup>3-7</sup> In **Figure 11a**, the emission spectrum of original 18 nm cores is represented by a black line. The emission spectra of core-shell nanoparticles, represented by the four colored lines, exhibited higher fluorescence intensities at all three emission wavelengths compared to the cores, represented by the black line. Comparison of the colored lines indicate that the 35 nm doped core-undoped shell nanoparticles shown by the purple line had the highest intensity. Comparing to the red peak at 656 nm and green peak at 528 nm, the green peak at 542 nm has much higher intensity. In **Figure 11b**, the peak intensity was shown in function of shell thickness. From **Figure 11b**, the trend showed that as the shell thickness increased, the intensity gradually increased. The observed fluorescence intensity indicates that the upconversion energy transfer was enhanced by introducing a layer of undoped shell as a protecting layer. The shell separated the core with surface ligands and solvent molecules, which inhibited the nonradiative transition and the surface quenching on the surface of NaYF<sub>4</sub>:Yb<sub>0.20</sub>, Er<sub>0.02</sub> core nanoparticles.

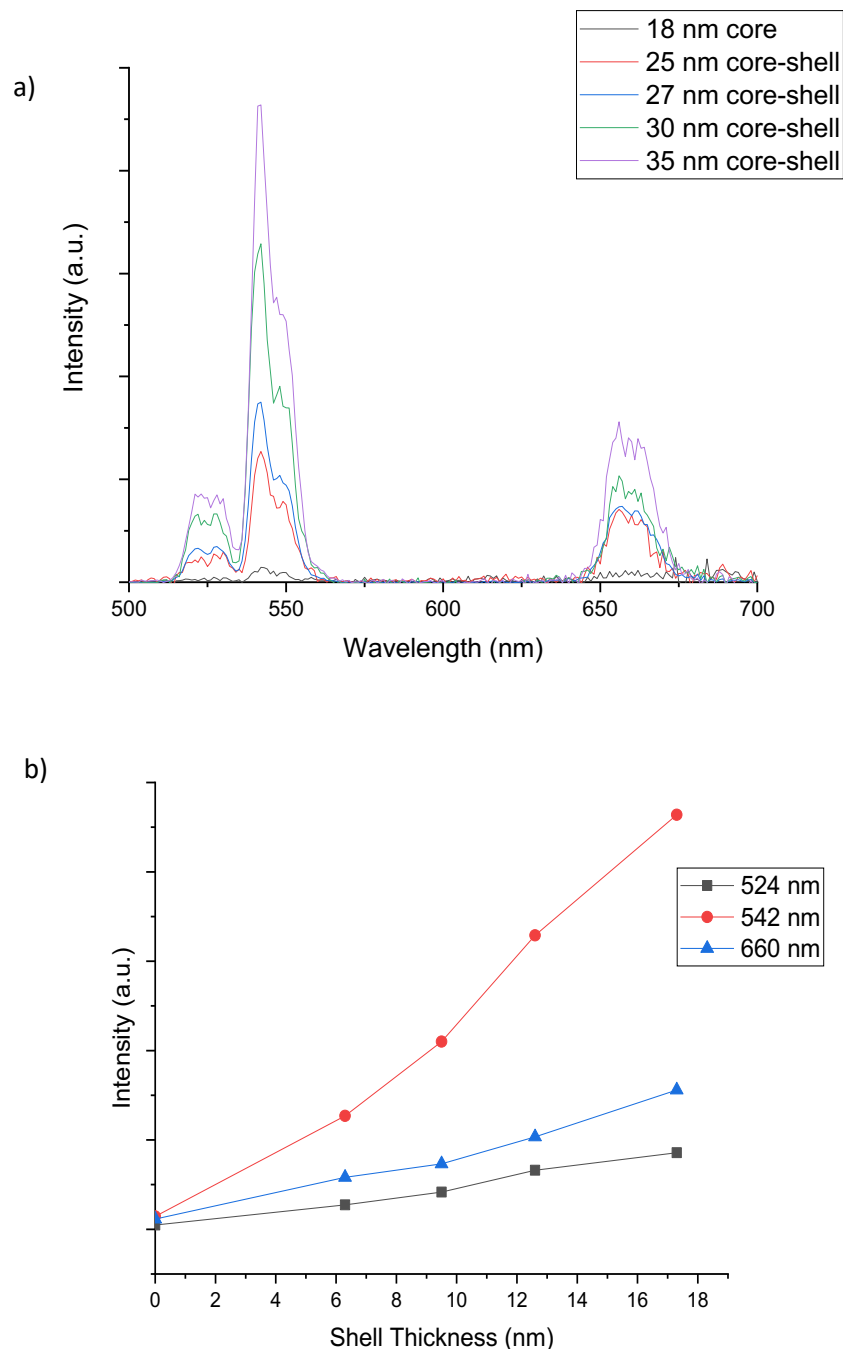


**Figure 11.** Emission spectrum of NaYF<sub>4</sub>:Yb<sub>0.20</sub>, Er<sub>0.02</sub> core nanoparticles and NaYF<sub>4</sub> doped core-undoped shell nanoparticles under 980 nm excitation. a) Up-conversion fluorescence under the 980 nm excitation; b) Up-conversion fluorescence intensity with respect of shell thickness.

In an attempt to further enhance the optical properties of NaYF<sub>4</sub>:Yb<sub>0.20</sub>, Er<sub>0.02</sub> core nanoparticles, CdS semiconductor and IR-806 dye were added to NaYF<sub>4</sub>:Yb<sub>0.20</sub>, Er<sub>0.02</sub> system. The 18 nm NaYF<sub>4</sub>:Yb<sub>0.20</sub>, Er<sub>0.02</sub> core nanoparticles were used to make

CdS/NaYF<sub>4</sub>:Yb<sub>0.20</sub>, Er<sub>0.02</sub> core-shell nanostructures and dye coated system via a solvothermal was used (**Figure 12**). Cadmium precursor and TOPO was heated to 340 °C in the presence of OA, a ligand to control the suspension of nanoparticles. At 340 °C, TOPO melted and became TOP solvent. When cadmium precursor dissolved in TOP, the solution became clear. Then, NaYF<sub>4</sub>:Yb<sub>0.20</sub>, Er<sub>0.02</sub> core nanoparticles were injected at 150 °C. The reaction was then heated to 350 °C in the presence of sulfur precursors to obtain the final product.

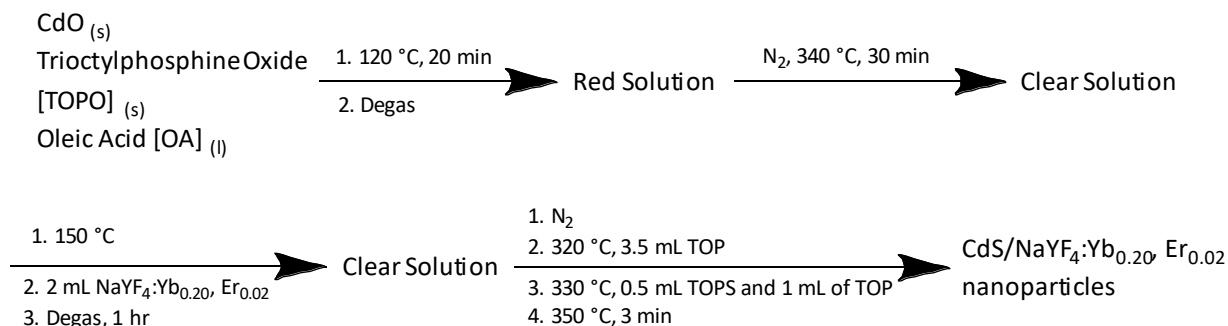


**Figure 12.** Synthesis of CdS/NaYF<sub>4</sub>:Yb<sub>0.20</sub>, Er<sub>0.02</sub>.<sup>24-26</sup>

TEM was used to characterize the morphology of the CdS/NaYF<sub>4</sub>:Yb<sub>0.20</sub>, Er<sub>0.02</sub> nanoparticles, as shown in **Figure 13**. The absorption and emission spectrum were performed at room temperature (**Figures 14-15**).

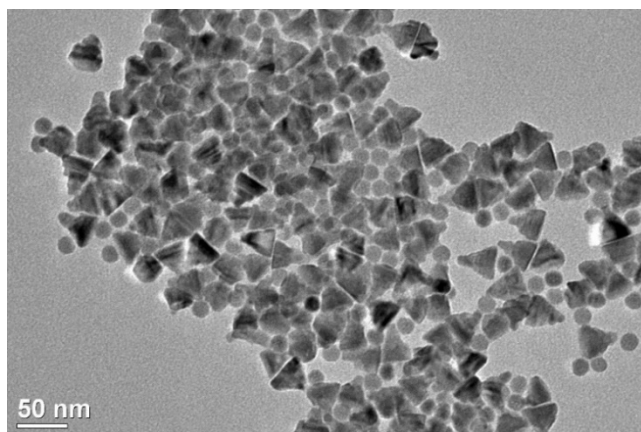


**Figure 13.** TEM image of CdS/NaYF<sub>4</sub>:Yb<sub>0.20</sub>, Er<sub>0.02</sub> nanoparticles.

In **Figure 13**, the size of spherical particles was  $17.8 \pm 1.6$  nm, while the size of triangular particles was  $29.4 \pm 2.4$  nm in width and  $33.2 \pm 4.7$  nm in height. The size and morphology of round particles indicated that these were unreacted NaYF<sub>4</sub>:Yb<sub>0.20</sub>, Er<sub>0.02</sub> core particles. From **Figure 13**, the triangular particles did not form a uniform shell on the surface of NaYF<sub>4</sub>:Yb<sub>0.20</sub>, Er<sub>0.02</sub> core nanoparticles. Instead, some of the triangular particles surrounded the round NaYF<sub>4</sub>:Yb<sub>0.20</sub>, Er<sub>0.02</sub> core particles, and some of the NaYF<sub>4</sub>:Yb<sub>0.20</sub>, Er<sub>0.02</sub> core particles merged into the triangular particles. The TEM image indicated that CdS/NaYF<sub>4</sub>:Yb<sub>0.20</sub>, Er<sub>0.02</sub> formed heterostructures instead of core-shell structure. Then, absorption and emission spectra were measured to study the optical properties of synthesized CdS/NaYF<sub>4</sub>:Yb<sub>0.20</sub>, Er<sub>0.02</sub> heterostructures.

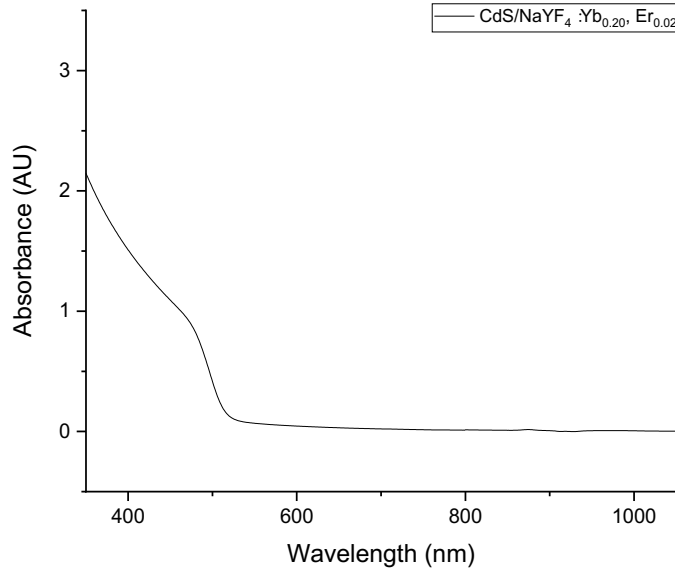


**Figure 14.** Absorption spectrum of CdS/NaYF<sub>4</sub>:Yb<sub>0.20</sub>, Er<sub>0.02</sub> heterostructure dispersed in hexane.

**Figure 14** shows the absorption spectrum of CdS/NaYF<sub>4</sub>:Yb<sub>0.20</sub>, Er<sub>0.02</sub> heterostructure. A wide absorption band was observed starting 500 nm and reaching to UV range. This can be assigned to UV-vis absorption from CdS, as compared to the literature.<sup>25,33,34</sup> However, the absorption of undiluted CdS/NaYF<sub>4</sub>:Yb<sub>0.20</sub>, Er<sub>0.02</sub> heterostructure at 980 nm was an order of magnitude lower than diluted NaYF<sub>4</sub>:Yb<sub>0.20</sub>, Er<sub>0.02</sub> core and NaYF<sub>4</sub> doped core-undoped shell nanoparticles (0.052 AU comparing to 0.006 AU). Such a low absorption indicated that the Yb<sup>3+</sup> ion did not have sufficient absorption in CdS/NaYF<sub>4</sub>:Yb<sub>0.20</sub>, Er<sub>0.02</sub> heterostructure.

The emission spectrum was measured under 980 nm excitation (**Figure 15**). The black line represents the emission spectrum of 18 nm NaYF<sub>4</sub>:Yb<sub>0.20</sub>, Er<sub>0.02</sub> core nanoparticles. The red line represents the emission spectrum of CdS/NaYF<sub>4</sub>:Yb<sub>0.20</sub>, Er<sub>0.02</sub> heterostructure. There was no significant absorption or emission observed for the CdS/NaYF<sub>4</sub>:Yb<sub>0.20</sub>, Er<sub>0.02</sub> heterostructure. (980nm excitation), compared to 18 nm NaYF<sub>4</sub>:Yb<sub>0.20</sub>, Er<sub>0.02</sub> core nanoparticles. This is further evidence that the target core-shell structures were not formed.



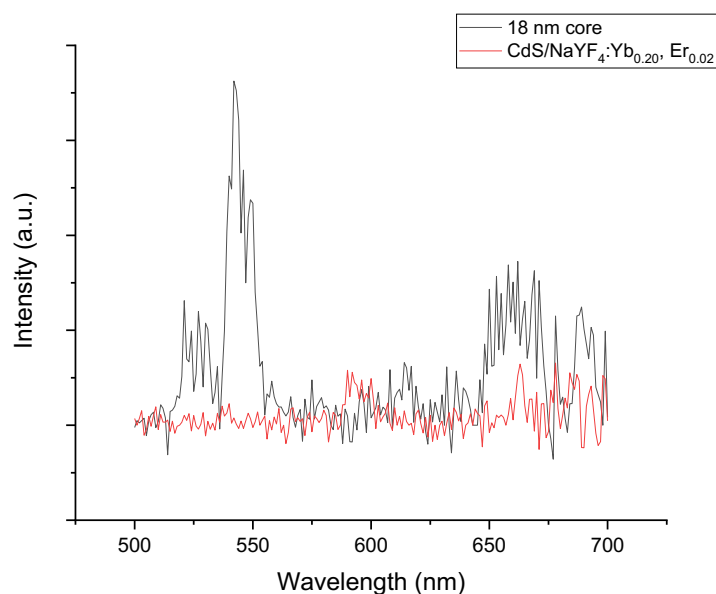


**Figure 15.** Emission spectrum of 18 nm NaYF<sub>4</sub>:Yb<sub>0.20</sub>, Er<sub>0.02</sub> core and CdS/NaYF<sub>4</sub>:Yb<sub>0.20</sub>, Er<sub>0.02</sub> heterostructure under the 980 nm excitation.

A ligand exchange approach was also used to coat IR-806 dye to the 18 nm NaYF<sub>4</sub>:Yb<sub>0.20</sub>, Er<sub>0.02</sub> core nanoparticles as another attempt to enhance the optical properties. The nanoparticles suspension changed from transparent to red. The optical properties of both dye solution and dye/NaYF<sub>4</sub>:Yb<sub>0.20</sub>, Er<sub>0.02</sub> system was investigated at room temperature.

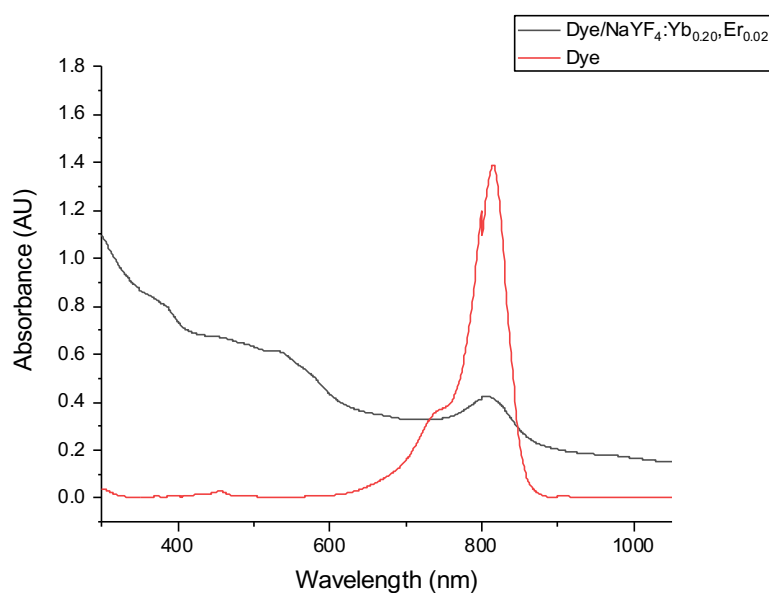


**Figure 16.** Absorption spectrum of IR-806 dye dissolved in 3:1 solvent of isopropanol and ethanol, and dye/NaYF<sub>4</sub>:Yb<sub>0.20</sub>, Er<sub>0.02</sub> nanoparticles dispersed in same solvent.

In **Figure 16**, the red line was the absorption of dye solution in 3:1 solution of isopropanol and ethanol, while the black line was the absorption of dye/NaYF<sub>4</sub>:Yb<sub>0.20</sub>, Er<sub>0.02</sub> nanoparticles. The dye solution has a very strong absorption band at about 804 nm, which was expected as the IR-806 dye had a strong absorption at 800-806 nm range. The dye/NaYF<sub>4</sub>:Yb<sub>0.20</sub>, Er<sub>0.02</sub> nanoparticles had absorption peak at 804 nm, which was expected from the coated dye. The absorption spectrum also revealed that dye/NaYF<sub>4</sub>:Yb<sub>0.20</sub>, Er<sub>0.02</sub> nanoparticles had strong absorption bands from 300-600 nm. The absorption peak at 520 nm was due to the absorption of Er<sup>3+</sup> in NaYF<sub>4</sub>:Yb<sub>0.20</sub>, Er<sub>0.02</sub> core nanoparticles. The absorption spectrum explained the color change of the nanoparticles. In visible range (380-750 nm), dye solution had absorption in red zone (620-750 nm). As a complementary color of red, green was observed in dye solution. Meanwhile, dye/NaYF<sub>4</sub>:Yb<sub>0.20</sub>, Er<sub>0.02</sub> core nanoparticles had strong absorption in 380-650 nm, which left weak absorption in red zone (650-720). Thus, red was observed in dye/NaYF<sub>4</sub>:Yb<sub>0.20</sub>, Er<sub>0.02</sub> nanoparticles rather than green. Based on absorption spectrum, the dye/NaYF<sub>4</sub>:Yb<sub>0.20</sub>, Er<sub>0.02</sub> nanoparticles had absorption peak at 804 nm. The emission spectrum of dye-coated system was then performed under 804 nm excitation.

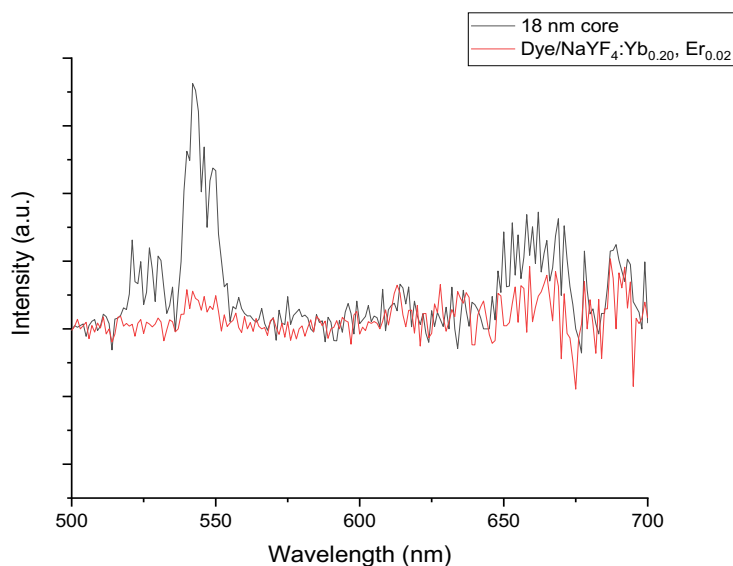


**Figure 17.** Emission spectrum of dye/NaYF<sub>4</sub>:Yb<sub>0.20</sub>, Er<sub>0.02</sub> nanoparticles (red) and 18 nm NaYF<sub>4</sub>:Yb<sub>0.20</sub>, Er<sub>0.02</sub> core nanoparticles (black) under the 804 nm excitation.

The emission spectra of dye/NaYF<sub>4</sub>:Yb<sub>0.20</sub>, Er<sub>0.02</sub> were performed under 804 nm excitation. In **Figure 17**, black line represented the emission of 18 nm NaYF<sub>4</sub>:Yb<sub>0.20</sub>, Er<sub>0.02</sub> core nanoparticles, while the red line represented the emission of dye/NaYF<sub>4</sub>:Yb<sub>0.20</sub>, Er<sub>0.02</sub> system. Compared to the 18 nm core, the dye-coated system did not have stronger emission intensity at 524 nm, 542 nm and 660 nm. However, the absorption spectrum and the color change after ligand exchange indicated that there might be interaction between IR-806 dye and NaYF<sub>4</sub>:Yb<sub>0.20</sub>, Er<sub>0.02</sub> core nanoparticles.

## Conclusion

In this project, both NaYF<sub>4</sub>:Yb<sub>0.20</sub>, Er<sub>0.02</sub> core and NaYF<sub>4</sub> doped core-undoped shell nanoparticles were synthesized in controlled sizes and quality by the solvothermal method and characterized by TEM and XRD. The sizes of NaYF<sub>4</sub>:Yb<sub>0.20</sub>, Er<sub>0.02</sub> core nanoparticles were ranging from 18-22 nm. Different sizes of undoped NaYF<sub>4</sub> shells (7 nm, 10 nm, 12 nm and 17 nm) were grown on the 18 nm NaYF<sub>4</sub>:Yb<sub>0.20</sub>, Er<sub>0.02</sub> core nanoparticles to form NaYF<sub>4</sub> doped core-undoped shell nanoparticles as an attempt to enhance the optical emission. The absorption and emission spectra of NaYF<sub>4</sub>:Yb<sub>0.20</sub>, Er<sub>0.02</sub> core and NaYF<sub>4</sub> doped core-undoped shell nanoparticles were measured at room temperature. From the emission spectrum, a sharp absorption peak was observed at 980 nm, which corresponded to the absorption from Yb<sup>3+</sup> ion. Weak peaks were also observed at 528 nm, 542 nm, and 660 nm, which corresponded to the excitation of Er<sup>3+</sup> ion from ground state to the excited state. The emission spectra were measured under 980 nm excitation. The emission peaks were found at 528 nm, 542 nm and 660 nm, which corresponded to emissions from Er<sup>3+</sup> ion. The NaYF<sub>4</sub> doped core-undoped shell nanoparticles had stronger emission intensity over NaYF<sub>4</sub>:Yb<sub>0.20</sub>, Er<sub>0.02</sub> core nanoparticles. The emission intensity gradually intensified as the shell thickness increases from 7 nm to 17 nm. This was presumably because the undoped shell performed as a protecting layer and inhibited the surface quenching effect by separating the surface of doped NaYF<sub>4</sub>:Yb<sub>0.20</sub>, Er<sub>0.02</sub> core with OA ligand and solvent. CdS semiconductor and IR-806 dye was added to NaYF<sub>4</sub>:Yb<sub>0.20</sub>, Er<sub>0.02</sub> core as an attempt to enhance the optical absorptions. CdS/NaYF<sub>4</sub>:Yb<sub>0.20</sub>, Er<sub>0.02</sub> system was prepared by another solvothermal method. TEM characterization indicated that CdS and NaYF<sub>4</sub>:Yb<sub>0.20</sub>, Er<sub>0.02</sub> formed heterostructure instead of core-shell structure. The absorption spectrum revealed that the absorption of CdS was predominated in CdS/NaYF<sub>4</sub>:Yb<sub>0.20</sub>, Er<sub>0.02</sub> heterostructure. According to absorption and emission spectra, CdS/NaYF<sub>4</sub>:Yb<sub>0.20</sub>, Er<sub>0.02</sub> heterostructure did not have better optical properties under 980 nm excitation. IR-806 dye was coated to NaYF<sub>4</sub>:Yb<sub>0.20</sub>, Er<sub>0.02</sub> core nanoparticles by ligand exchange method. The absorption spectrum confirmed that the dye/NaYF<sub>4</sub>:Yb<sub>0.20</sub>, Er<sub>0.02</sub> nanoparticles absorbed strongly in 380-650 nm and 800-804 nm ranges. It also revealed that the red color of dye/NaYF<sub>4</sub>:Yb<sub>0.20</sub>, Er<sub>0.02</sub> nanoparticles was due to the weak absorption at red zone (650-720). The absorption spectrum indicated that the dye enhanced the optical absorption of dye/NaYF<sub>4</sub>:Yb<sub>0.20</sub>, Er<sub>0.02</sub> nanoparticles in 804 nm.

## Future Work

To study the limit of the shell thickness to the optical properties, thicker undoped NaYF<sub>4</sub> shells can be grown on the NaYF<sub>4</sub>:Yb<sub>0.20</sub>, Er<sub>0.02</sub> core particles. Other semiconductors, such as CdSe, ZnS, PbS, can be tried as upconversion sensitizers for semiconductor sensitized nanoparticles. Other than semiconductors, more detailed studied for energy transfer between the dye and nanoparticles is needed, especially the emission properties of dye/NaYF<sub>4</sub>:Yb<sub>0.20</sub>, Er<sub>0.02</sub> nanoparticles under NIR excitation. IR-806 dye is soluble in water. An optimized synthetic method or ligand exchange conditions can be studied to make IR-806 dye/NaYF<sub>4</sub>:Yb<sub>0.20</sub>, Er<sub>0.02</sub> nanoparticles soluble in water. Meanwhile, more organic dyes can be tried other than IR-806. Lastly, the downconversion of the NaYF<sub>4</sub>:Yb<sub>0.20</sub>, Er<sub>0.02</sub> core nanoparticles can be studied with 377 nm excitation.

## References

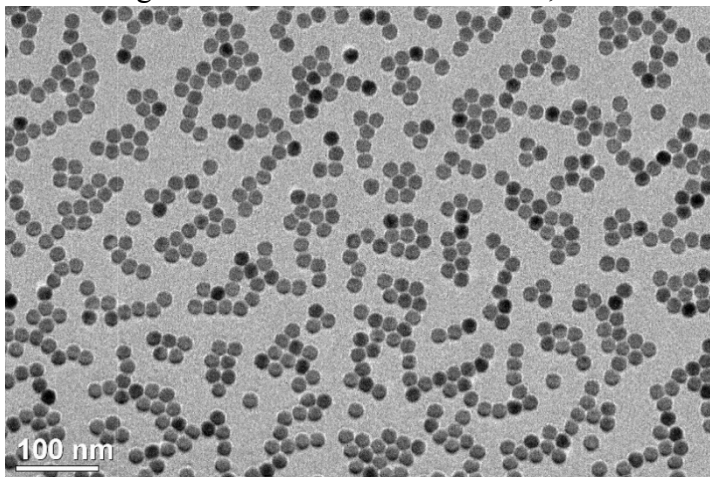
- (1) Turro, N. J.; Ramamurthy, V.; Scaiano, J. C. *Principles of molecular photochemistry: an introduction*; University Science Books: Sausalito, CA, 2009.
- (2) Najmr, S. Synthesis, Surface Treatment, and 3D Visualization of Anisotropic and Multifunctional Rare-Earth Nanocrystals. Ph.D Thesis, University of Pennsylvania, Philadelphia, PA, 2018.
- (3) *Multiple chemical sensitivities addendum to Biologic markers in immunotoxicology*; National Academy Press: Washington, D.C., 1992.
- (4) Trupke, T.; Green, M. A.; Würfel, P. Improving solar cell efficiencies by up-conversion of sub-band-gap light. *J. Appl. Phys.* **2002**, 92.
- (5) Mai, H. X.; Zhang, Y. W.; Sun, L. D.; Yan, C. H. *J. Phys. Chem. C* **2007**, 111, 13730–13739.
- (6) Qin, H.; Wu, D.; Sathian, J.; Xie, X.; Ryan, M.; Xie, F. Tuning the upconversion photoluminescence lifetimes of NaYF<sub>4</sub>:Yb<sup>3+</sup>, Er<sup>3+</sup> through lanthanide Gd<sup>3+</sup> doping. *Scientific Reports.* **2018**, 8, (1).
- (7) Ye, S.; Xiao, P.; Liao, H.; Li, S.; Wang, D. Fast synthesis of sub-10 nm  $\beta$ -NaYF<sub>4</sub>:Yb<sup>3+</sup>,Er<sup>3+</sup>@NaYF<sub>4</sub> core-shell upconversion nanocrystals mediated by oleate ligands. *Mater. Res. Bull.* **2018**, 103, 279–284.
- (8) Joubert, M. F. Photon avalanche upconversion in rare earth laser materials. *Opt. Mater.* **1999**, 11, 181–203.
- (9) Wang, J.; Deng, R. Energy Transfer in Dye-Coupled Lanthanide-Doped Nanoparticles: From Design to Application. *Chem. Asian J.* **2018**, 13, 614 – 625.
- (10) Tan, L.; Ke, X.; Song, X.; Yin, Q.; Qiao, R.; Guo, K.; Zhu, L. Double-layered core-shell structure of NaYF<sub>4</sub>:Yb,Er@SiO<sub>2</sub>@Zn<sub>1-x</sub>Mn<sub>x</sub>O for near-infrared-triggered photodegradation and antibacterial application. *Journal of Industrial and Engineering Chemistry.* **2018**, 60, 206–217.
- (11) Wang, Z.; Li, J.; Zhu, Q.; Li, X.; Sun, X. Hydrothermal conversion of layered hydroxide nanosheets into (Y<sub>0.95</sub>Eu<sub>0.05</sub>)PO<sub>4</sub> and (Y<sub>0.96-x</sub>Tb<sub>0.04</sub>Eu<sub>x</sub>)PO<sub>4</sub> (x = 0–0.10) nanocrystals for red and color-tailorable emission. *RSC Adv.* **2016**, 6, 22690–22699.
- (12) Sun, J.; Mi, X.; Lei, L.; Pan, X.; Chen, S.; Wang, Z.; Bai, Z.; Zhang, X. Hydrothermal synthesis and photoluminescence properties of Ca<sub>9</sub>Eu(PO<sub>4</sub>)<sub>7</sub> nanophosphors. *Cryst. Eng. Comm.* **2015**, 17, 7888–7895.
- (13) Mai, H.; Zhang, Y.; Sun, L.; Yan, C. Size- and Phase-Controlled Synthesis of Monodisperse NaYF<sub>4</sub>:Yb,Er Nanocrystals from a Unique Delayed Nucleation Pathway Monitored with Upconversion Spectroscopy. *J. Phys. Chem. C* **2007**, 111 (37), 13730–13739.
- (14) Klier, D. T.; Kumke, M. U. Analyzing the effect of the crystal structure on upconversion luminescence in Yb<sup>3+</sup>, Er<sup>3+</sup>-co-doped NaYF<sub>4</sub> nanomaterials. *J. Mater. Chem. C.* **2015**, 3, 11228–11238.
- (15) Liu, J.; Liu, X.; Kong, X.; Zhang, H. Controlled synthesis, formation mechanism and upconversion luminescence of NaYF<sub>4</sub>: Yb, Er nano-/submicrocrystals via ionothermal approach. *J. Solid State Chem.* **2012**, 190, 98–103.
- (16) Liu, X.; Zhao, J.; Sun, Y.; Song, K.; Yu, Y.; Du, C.; Kong, X.; Zhang, H. Ionothermal synthesis of hexagonal-phase NaYF<sub>4</sub>:Yb<sup>3+</sup>,Er<sup>3+</sup>/Tm<sup>3+</sup> upconversion nanophosphors. *Chem. Commun.* **2009**, 6628–6630.

- (17) Ju, Q.; Campbell, P. S.; Mudring, A. Interface-assisted ionothermal synthesis, phase tuning, surface modification and bioapplication of  $\text{Ln}^{3+}$ -doped  $\text{NaGdF}_4$  nanocrystals. *J. Mater. Chem. B*. **2013**, *1*, 179–185.
- (18) Cooper, E. R.; Andrews, C. D.; Wheatley, P. S.; Webb, P. B.; Wormald, P.; Morris, R. E. Ionic liquids and eutectic mixtures as solvent and template in synthesis of zeolite analogues. *Nature*. **2004**, *430* (August), 1012–1016.
- (19) Lemyre, J. L.; Ritcey, A. M. Synthesis of Lanthanide Fluoride Nanoparticles of Varying Shape and Size. *Chem. Mater.* **2005**, *17* (11), 3040–3043.
- (20) Mai, H.; Zhang, Y.; Si, R.; Yan, Z.; Sun, L.; You, L.; Yan, C. High-Quality Sodium Rare-Earth Fluoride Nanocrystals: Controlled Synthesis and Optical Properties. *J. Am. Chem. Soc.* **2006**, *128*, 19, 6426–6436.
- (21) Fang, Y.; Xu, A.; Song, R.; Zhang, H.; You, L.; Yu, J. C.; Liu, H. Systematic Synthesis and Characterization of Single-Crystal Lanthanide Orthophosphate Nanowires. *J. Am. Chem. Soc.* **2003**, *125* (6), 16025–16034.
- (22) Wang, Z. L.; Hao, J.; Chan, H. L. W.; Wong, W. T.; Wong, K. L. A Strategy for Simultaneously Realizing the Cubic-to-Hexagonal Phase Transition and Controlling the Small Size of  $\text{NaYF}_4\text{:Yb}^{3+},\text{Er}^{3+}$  Nanocrystals for In Vitro Cell Imaging. *Small*. **2012**, *8*, 1863–1868.
- (23) Auzel, F.; Pecile, D. Comparison and Efficiency of Materials for Summation of Photons Assisted by Energy Transfer. *Journal of Luminescence*. **1973**, *8* (1), 32–43.
- (24) C. B. Murray, D. J. Norris, and M. G. Bawendi. Synthesis and characterization of nearly monodisperse  $\text{CdE}$  ( $\text{E} = \text{sulfur, selenium, tellurium}$ ) semiconductor nanocrystallites. *J. Am. Chem. Soc.* **1993**, *115* (19), 8706–8715.
- (25) Talapin, D. V.; Nelson, J. H.; Shevchenko, E. V.; Aloni, S.; Sadtler, B.; Alivisatos, A. P. Seeded Growth of Highly Luminescent  $\text{CdSe/CdS}$  Nanoheterostructures with Rod and Tetrapod Morphologies. *Nano Letters*. **2007**, *7* (10), 2951–2959.
- (26) Peng, Z. A.; Peng, X. Composition-Tunable  $\text{Zn}_x\text{Cd}_{1-x}\text{Se}$  Nanocrystals with High Luminescence and Stability. *ChemInform*. **2001**, *32* (14).
- (27) Dong, A.; Ye, X.; Chen, J.; Kang, Y.; Gordon, T.; Kikkawa, J. M.; Murray, C. B. A Generalized Ligand-Exchange Strategy Enabling Sequential Surface Functionalization of Colloidal Nanocrystals. *J. Am. Chem. Soc.* **2011**, *133* (4), 998–1006.
- (28) Sigma-Aldrich IR-806.  
[https://www.sigmaaldrich.com/catalog/product/aldrich/543349?lang=en&region=US&gclid=Cj0KCQjwh6XmBRDRARIsAKNIInDFwvsWviVsN7CGF\\_vkt8IbTOWvTVpBRd7\\_76IK0\\_BUzZSM6kPqL2AwaAoMDEALw\\_wcB](https://www.sigmaaldrich.com/catalog/product/aldrich/543349?lang=en&region=US&gclid=Cj0KCQjwh6XmBRDRARIsAKNIInDFwvsWviVsN7CGF_vkt8IbTOWvTVpBRd7_76IK0_BUzZSM6kPqL2AwaAoMDEALw_wcB) (accessed Mar. 17, 2019).
- (29) Beane, G.; Boldt, K.; Kirkwood, N.; Mulvaney, P. Energy Transfer between Quantum Dots and Conjugated Dye Molecules. *J. Phys. Chem. C*. **2014**, *118* (31), 18079–18086.
- (30) Artemyev, M.; Ustinovich, E.; Nabiev, I. Efficiency of Energy Transfer from Organic Dye Molecules to  $\text{CdSe-ZnS}$  Nanocrystals: Nanorods versus Nanodots. *J. Am. Chem. Soc.* **2009**, *131* (23), pp 8061–8065.
- (31) Perera, S. S.; Amarasinghe, D. K.; Dissanayake, K. T.; Rabuffetti, F. A. Average and local crystal structure of  $\beta\text{-Er:Yb:NaYF}_4$  upconverting nanocrystals probed by X-ray total scattering. *Chem. Mater.* **2017**, *29* (15), 6289–6297.
- (32) *Inorganic Crystal Structure Database (ICSD)*; XRD pattern; Collection Code 259178; <https://proxy.library.upenn.edu:3971/display/details.xhtml> (accessed Feb. 22, 2019).

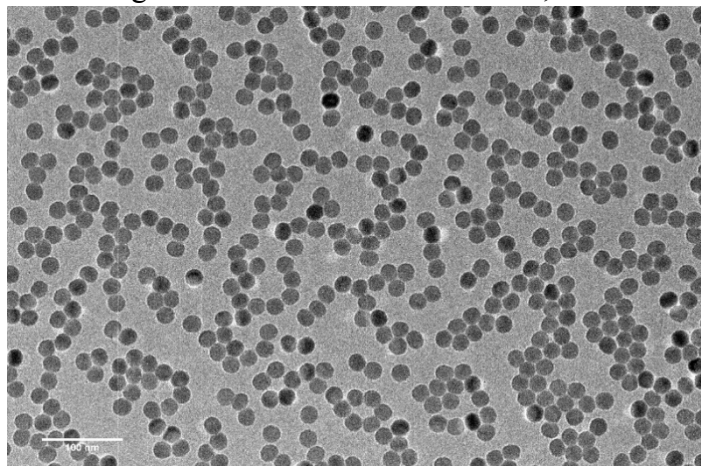
- (33) Singh, N.; Mehra, R. M.; Kapoor, A.; Soga, T. ZnO based quantum dot sensitized solar cell using CdS quantum dots. *J. Renewable Sustainable Energy*. **2012**, *4* (1), 013110.
- (34) Warner, J. H.; Tilley, R. D. Synthesis and Self-Assembly of Triangular and Hexagonal CdS Nanocrystals. *Adv. Mater.* **2005**, *17*, 2997–3001.

## Appendices

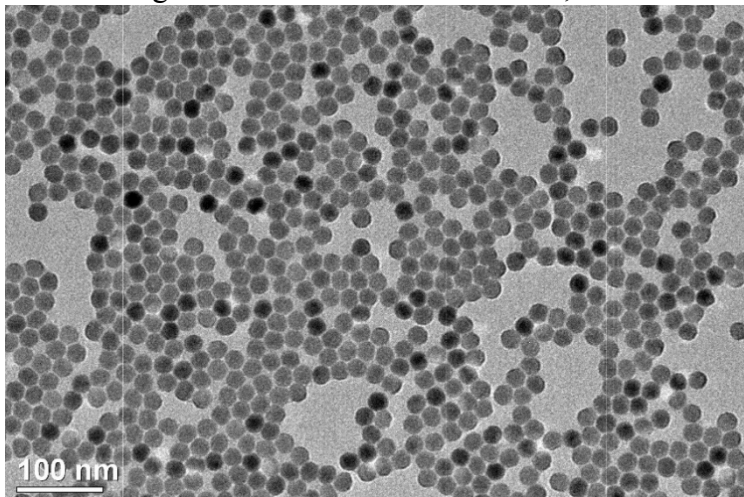
**Appendix 1.** TEM images of 18 nm core NaYF<sub>4</sub>:Yb<sub>0.20</sub>, Er<sub>0.02</sub> core nanoparticles.



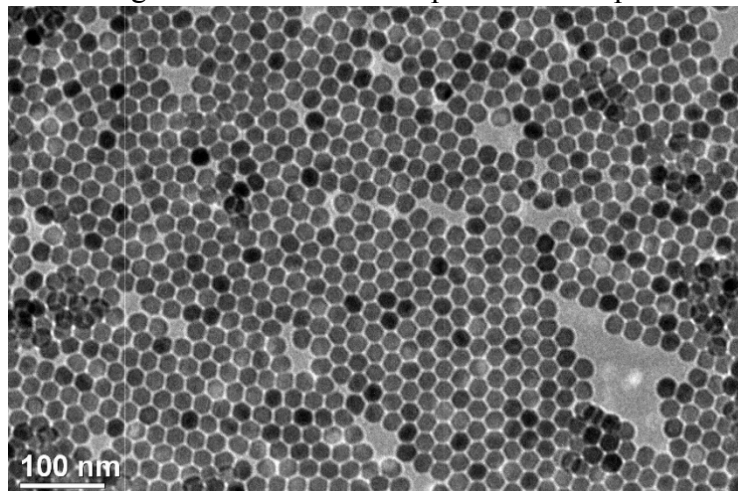
**Appendix 2.** TEM images of 20 nm core NaYF<sub>4</sub>:Yb<sub>0.20</sub>, Er<sub>0.02</sub> core nanoparticles.



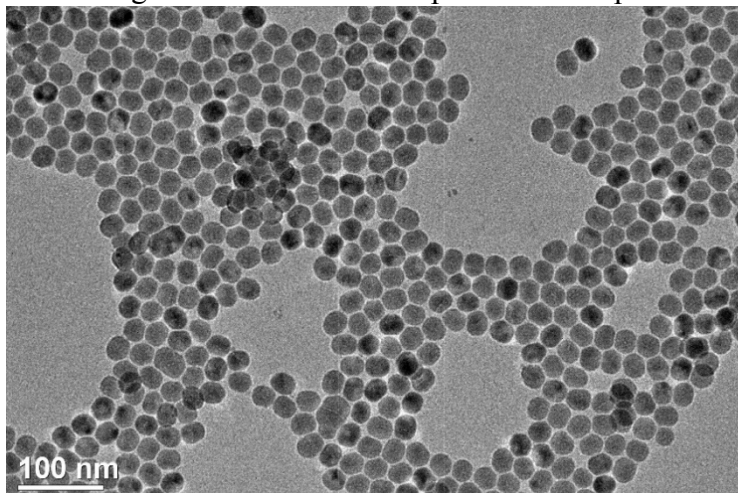
**Appendix 3.** TEM images of 22 nm core NaYF<sub>4</sub>:Yb<sub>0.20</sub>, Er<sub>0.02</sub> core nanoparticles.



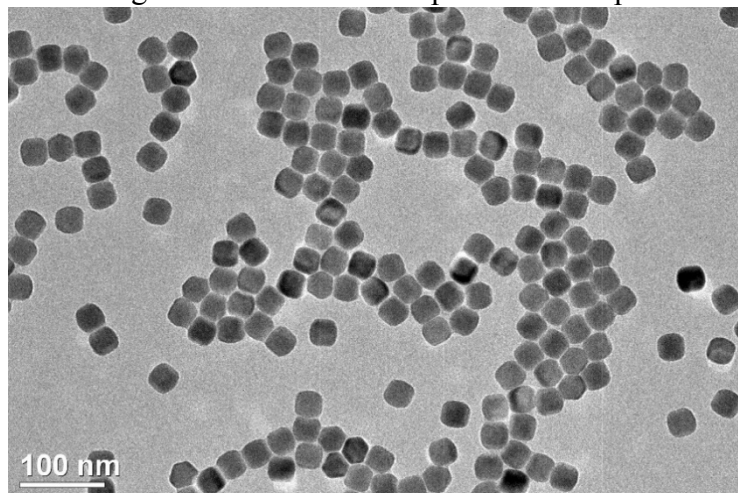
**Appendix 4.** TEM images of 25 nm NaYF<sub>4</sub> doped core-undoped shell nanoparticles.



**Appendix 5.** TEM images of 28 nm NaYF<sub>4</sub> doped core-undoped shell nanoparticles.

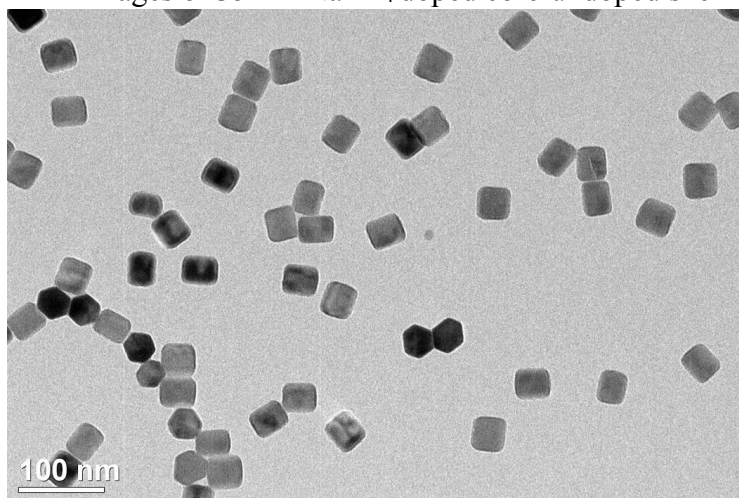


**Appendix 6.** TEM images of 30 nm NaYF<sub>4</sub> doped core-undoped shell nanoparticles.

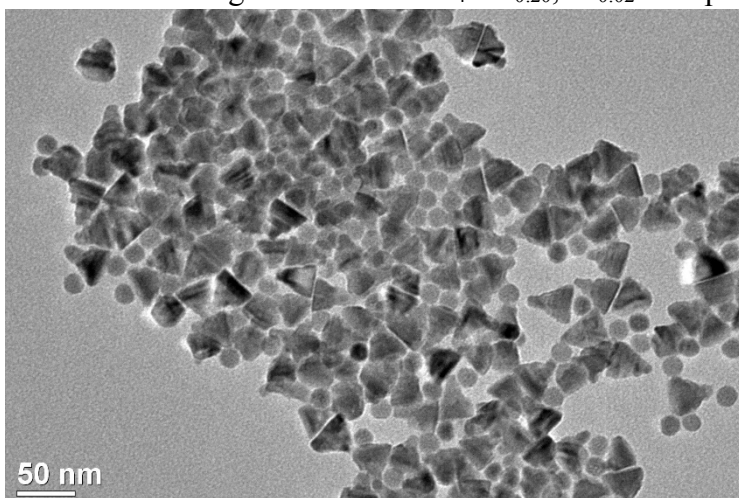




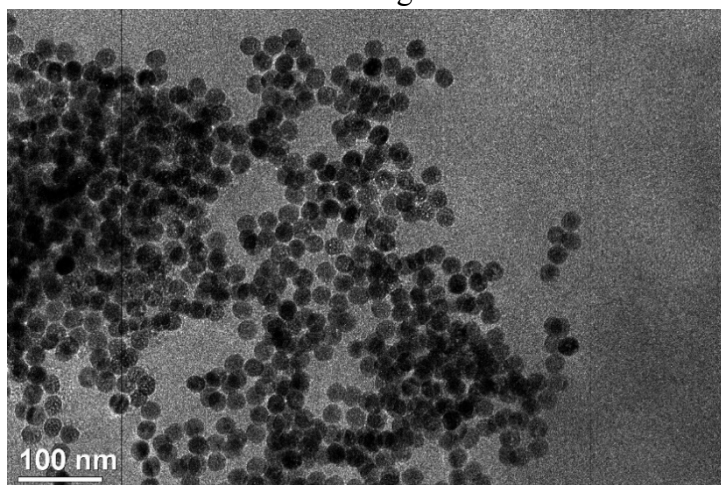
**Appendix 7.** TEM images of 35 nm NaYF<sub>4</sub> doped core-undoped shell nanoparticles.



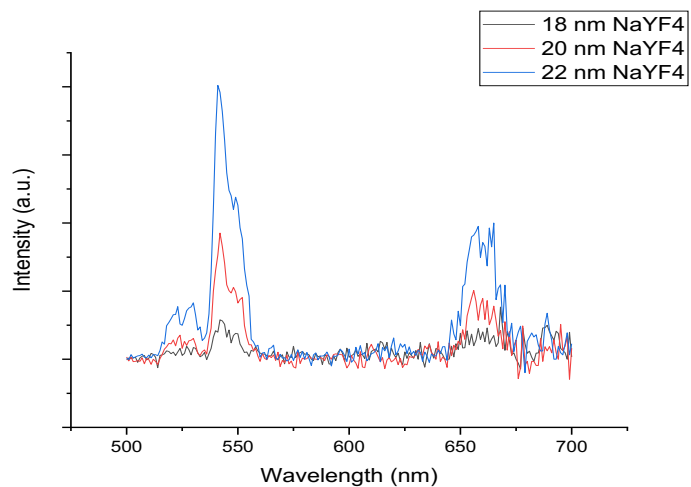
**Appendix 8.** TEM images of CdS/NaYF<sub>4</sub>:Yb<sub>0.20</sub>, Er<sub>0.02</sub> nanoparticles.



**Appendix 9.** TEM images of Dye/NaYF<sub>4</sub>:Yb<sub>0.20</sub>, Er<sub>0.02</sub> nanoparticles after ligand exchange



**Appendix 10.** Emission spectra of NaYF<sub>4</sub>:Yb<sub>0.20</sub>, Er<sub>0.02</sub> core nanoparticles.



**Appendix 11.** Hexane suspension of 18 nm NaYF<sub>4</sub>:Yb<sub>0.20</sub>, Er<sub>0.02</sub> core nanoparticles (left);  
Hexane suspension of CdS/NaYF<sub>4</sub>:Yb<sub>0.20</sub>, Er<sub>0.02</sub> (right).



**Appendix 12.** Hexane suspension of 18 nm NaYF<sub>4</sub>:Yb<sub>0.20</sub>, Er<sub>0.02</sub> core nanoparticles (left);  
IR-806 dye dissolved in 3:1 solvent of isopropanol and ethanol (middle);  
Dye/NaYF<sub>4</sub>:Yb<sub>0.20</sub>, Er<sub>0.02</sub> nanoparticles dispersed in toluene (right)

